OAA TECHNICAL MEMORANDUM NWS CR-109

SYNOPTIC, MESOSCALE AND RADAR ASPECTS OF THE NORTHEAST KANSAS SUPERCELL OF SEPTEMBER 21, 1993

Kenneth M. Labas
National Weather Service Forecast Office (Chicago)
Romeoville, Illinois

Brian P. Walawender
National Weather Service Forecast Office
Topeka, Kansas

October 1995

U.S DEPARTMENT OF Commerce / National Oceanic and Atmospheric Administration / National Weather Service

NOAA TECHNICAL MEMORANDA
National Weather Service, Central Region Subseries

The National Weather Service Central Region (CR) subseries provides an informal medium for the documentation and quick dissemination of results not appropriate, or not yet ready, for formal publication. The series is used to report on work in progress, to describe technical procedures and practices, or to relate progress to a limited audience. These Technical Memoranda report on investigations devoted primarily to regional and local problems of interest mainly to regional personnel, and hence will not be widely distributed.

Papers 1 through 15 are in the former series, ESSA Technical Memoranda, Central Region Technical Memoranda (CRTM); Papers 16 through 36 are in the former series, ESSA Technical Memoranda, Weather Bureau Technical Memoranda (WBTM). Beginning with Paper 37, the papers are part of the series, NOAA Technical Memoranda NWS.

Papers that have a PB or COM number are available from the National Technical Information Service, U. S. Department of Commerce, 5285 Port Royal Road, Springfield, VA 22151. Order by accession number shown in parenthesis at the end of each entry. Prices vary for all paper copies. Microfiche are $4.50. All other papers are available from the National Weather Service Central Region, Scientific Services, Room 1836, 601 East 12th Street, Kansas City, MO 64106.

ESSA Technical Memoranda

CRTM 1 Precipitation Probability Forecast Verification Summary Nov. 1965 - Mar. 1966, SSD Staff, WBCRH, May 1966.
CRTM 2 A Study of Summer Showers Over the Colorado Mountains. William G. Sullivan, Jr., and James O. Severson, June 1966.
CRTM 3 Areal Shower Distribution - Mountain Versus Valley Coverage. William G. Sullivan, Jr., and James O. Severson, June 1966.
CRTM 4 Heavy Rains in Colorado June 16 and 17, 1965. SSD Staff, WBCRH, July 1966.
CRTM 5 The Plum Fire. William G. Sullivan, Jr., August 1966.
CRTM 6 Precipitation Probability Forecast Verification Summary Nov. 1965 - July 1966. SSD Staff, WBCRH, September 1966.
CRTM 7 Effect of Diurnal Weather Variations on Soybean Harvest Efficiency. Leonard F. Hand, October 1966.
CRTM 8 Climatic Frequency of Precipitation at Central Region Stations. SSD Staff, WBCRH, November 1966.
CRTM 9 Heavy Snow or Glazing. Harry W. Waldheuser, December 1966.
CRTM 10 Detection of a Weak Front by WSR-57 Radar. G. W. Polensky, December 1966.
CRTM 11 Public Probability Forecasts. SSD Staff, WBCRH, January 1967.
CRTM 12 Heavy Snow Forecasting in the Central United States (an Interim Report). SSD Staff, January 1967.
CRTM 13 Diurnal Surface Geostrophic Wind Variations Over the Great Plains. Wayne E. Sangster, March 1967.
CRTM 14 Forecasting Probability of Summertime Precipitation at Denver. Wm. G. Sullivan, Jr., and James O. Severson, March 1967.
CRTM 15 Improving Precipitation Probability Forecasts Using the Central Region Verification Printout. Lawrence A. Hughes, May 1967.
WBTM CR 16 Small-Scale Circulations Associated with Radiational Cooling. Jack R. Cooley, June 1967.
WBTM CR 17 Probability Verification Results (6-month and 18-month). Lawrence A. Hughes, June 1967.
WBTM CR 18 On the Use and Misuse of the Brier Verification Score. Lawrence A. Hughes, August 1967 (PB 175 771).
WBTM CR 19 Probability Verification Results (24 months). Lawrence A. Hughes, February 1968.
WBTM CR 20 Radar Prediction of the Topeka Tornado. Norman E. Prosser, April 1968.
WBTM CR 21 Wind Waves on the Great Lakes. Lawrence A. Hughes, May 1968.
WBTM CR 22 Seasonal Aspects of Probability Forecasts: 1. Summer. Lawrence A. Hughes, June 1968 (PB 185 733).
WBTM CR 23 Seasonal Aspects of Probability Forecasts: 2. Fall. Lawrence A. Hughes, September 1968 (PB 185 734).
WBTM CR 24 The Importance of Areal Coverage in Precipitation Probability Forecasting. John T. Curran and Lawrence A. Hughes, September 1968.
WBTM CR 25 Meteorological Conditions as Related to Air Pollution, Chicago, Illinois, April 12-13, 1963. Charles H. Swan, October 1968.
WBTM CR 26 Seasonal Aspects of Probability Forecasts: 3. Winter. Lawrence A. Hughes, December 1968 (PB 185 735).
WBTM CR 27 Seasonal Aspects of Probability Forecasts: 4. Spring. Lawrence A. Hughes, February 1969 (PB 185 736).
WBTM CR 28 Minimum Temperature Forecasting During Possible Frost Periods at Agricultural Weather Stations in Western Michigan. Marshall E. Soderberg, March 1969.
WBTM CR 29 An Aid for Tornado Warnings. Harry W. Waldheuser and Lawrence A. Hughes, April 1969.
WBTM CR 30 An Aid in Forecasting Significant Lake Snows. H. J. Rothrock, November 1969.
WBTM CR 31 A Forecast Aid for Boulder Winds. Wayne E. Sangster, February 1970.
WBTM CR 32 An Objective Method for Estimating the Probability of Severe Thunderstorms. Clarence L. David, February 1970.
WBTM CR 33 Kentucky Air-Soil Temperature Climatology. Clyde B. Lee, February 1970.
WBTM CR 34 Effective Use of Non-Structural Methods in Water Management. Verne Alexander, March 1970.
WBTM CR 35 A Note on the Categorical Verification of Probability Forecasts. Lawrence A. Hughes and Wayne E. Sangster, August 1970.
WBTM CR 36 A Comparison of Observed and Calculated Urban Mixing Depths. Donald E. Wuerch, August 1970.

NOAA Technical Memoranda NWS

NWS CR 37 Forecasting Maximum and Minimum Surface Temperatures at Topeka, Kansas, Using Guidance from the PE Numerical Prediction Model (FOUS). Morris S. Webb, Jr., November 1970 (COM 71 00118).
NWS CR 38 Snow Forecasting for Southeastern Wisconsin. Rheinhart W. Harms, November 1970 (COM 71-00019).
NWS CR 39 A Synoptic Climatology of Blizzards on the North-Central Plains of the United States. Robert E. Black, February 1971 (COM 71-00369).
NWS CR 40 Forecasting the Spring 1969 Midwest Snowmelt Floods. Herman F. Mondschein, February 1971 (COM 71-00489).
NWS CR 41 The Temperature Cycle of Lake Michigan 1. (Spring and Summer). Lawrence A. Hughes, April 1971 (COM 71-00545).
NWS CR 42 Dust Devil Meteorology. Jack R. Cooley, May 1971 (COM 71-00628).
NWS CR 43 Summer Shower Probability in Colorado as Related to Altitude. Alois G. Topil, May 1971 (COM 71-00712).
NWS CR 44 An Investigation of the Resultant Transport Wind Within the Urban Complex. Donald E. Wuerch, June 1971 (COM 71- 00766).
NWS CR 45 The Relationship of Some Cirrus Formations to Severe Local Storms. William E. Williams, July 1971 (COM 71- 00844).
NWS CR 46 The Temperature Cycle of Lake Michigan 2. (Fall and Winter). Lawrence A. Hughes, September 1971 (COM 71-01039).

(Continued on Back Cover)

NOAA TECHNICAL MEMORANDUM NWS CR-109

SYNOPTIC, MESOSCALE AND RADAR ASPECTS OF THE NORTHEAST KANSAS SUPERCELL OF SEPTEMBER 21, 1993

Kenneth M. Labas
National Weather Service Forecast Office (Chicago)
Romeoville, Illinois

Brian P. Walawender
National Weather Service Forecast Office
Topeka, Kansas

October 1995

UNITED STATES
DEPARTMENT OF COMMERCE
Ronald H. Brown
Secretary

National Oceanic and
Atmospheric Administration
D. James Baker
Under Secretary

National Weather
Service
Elbert W. Friday, Jr.
Assistant Administrator

Table of Contents

SYNOPTIC, MESOSCALE AND RADAR ASPECTS OF THE NORTHEAST KANSAS SUPERCELL OF SEPTEMBER 21, 1993

Kenneth M. Labas
National Weather Service Forecast Office, Chicago
Romeoville, Illinois

Brian P. Walawender
National Weather Service Forecast Office
Topeka, Kansas

1. INTRODUCTION

On September 21, 1993, a supercell thunderstorm developed over north-central Kansas, near Concordia (CNK), in proximity to a warm frontal boundary. The storm maintained its identity for over nine hours (21/1500 UTC - 22/0000 UTC) as it propagated to the east then southeast along the nearly stationary discontinuity. Numerous reports of large hail, damaging winds and small tornadoes were received. Six tornadoes of F0 intensity were observed mainly during the earlier stages of it's lifetime.

This case exhibited focused destabilization as a result of a rapid increase in sensible heat and moisture content in the lowest layers of the troposphere along a pre-existing frontal boundary. A weak short-wave trough near 400-mb helped increase buoyancy due to cooling and consequent steepening of mid level lapse rates.

The 1200 UTC Topeka hodograph was modified on the SHARP Work Station (Hart and Korotky 1991) to reflect VAD winds detected at the WSR-88D (30 nm west of Topeka). Thermodynamic data was adjusted to reflect observed conditions prior to storm passage at WSFO Topeka (TOP) (a wall cloud passed just north of the station). Using these modifications the storm environment showed a rapid change toward one very favorable for severe convection, easily falling within parameters for supercells as defined by Johns and Doswell (1992) and Johns et al (1990).

The first section of this paper will review storm history. Reference will be made to observed synoptic and mesoscale data, as well as prognostic tools defined through gridded model output utilizing the PCGRIDDS software package.

The second portion will discuss aspects of the event as seen through the WSR-88D Doppler imagery. Radar signatures will be related to reported severe

weather events as documented in "Storm Data". The system progressed through a full spectrum of evolution, from a classic supercell to "High Precipitation" (HP) storm (as noted by Doswell, et al 1990) finally obtaining bow echo characteristics. Concurrently, the severe weather produced sequenced from tornadic to heavy rain/hail to wind events.

2. SYNOPTIC EVOLUTION

At 1200 UTC 21 September 1993, a 500-mb trough was edging southward through the northern Rockies. The broad southwest flow from the southern Plateau into the western High Plains trailed a retreating ridge line over eastern Kansas (Figure 1). A series of thermal troughs were noted in an otherwise uniform flow field.

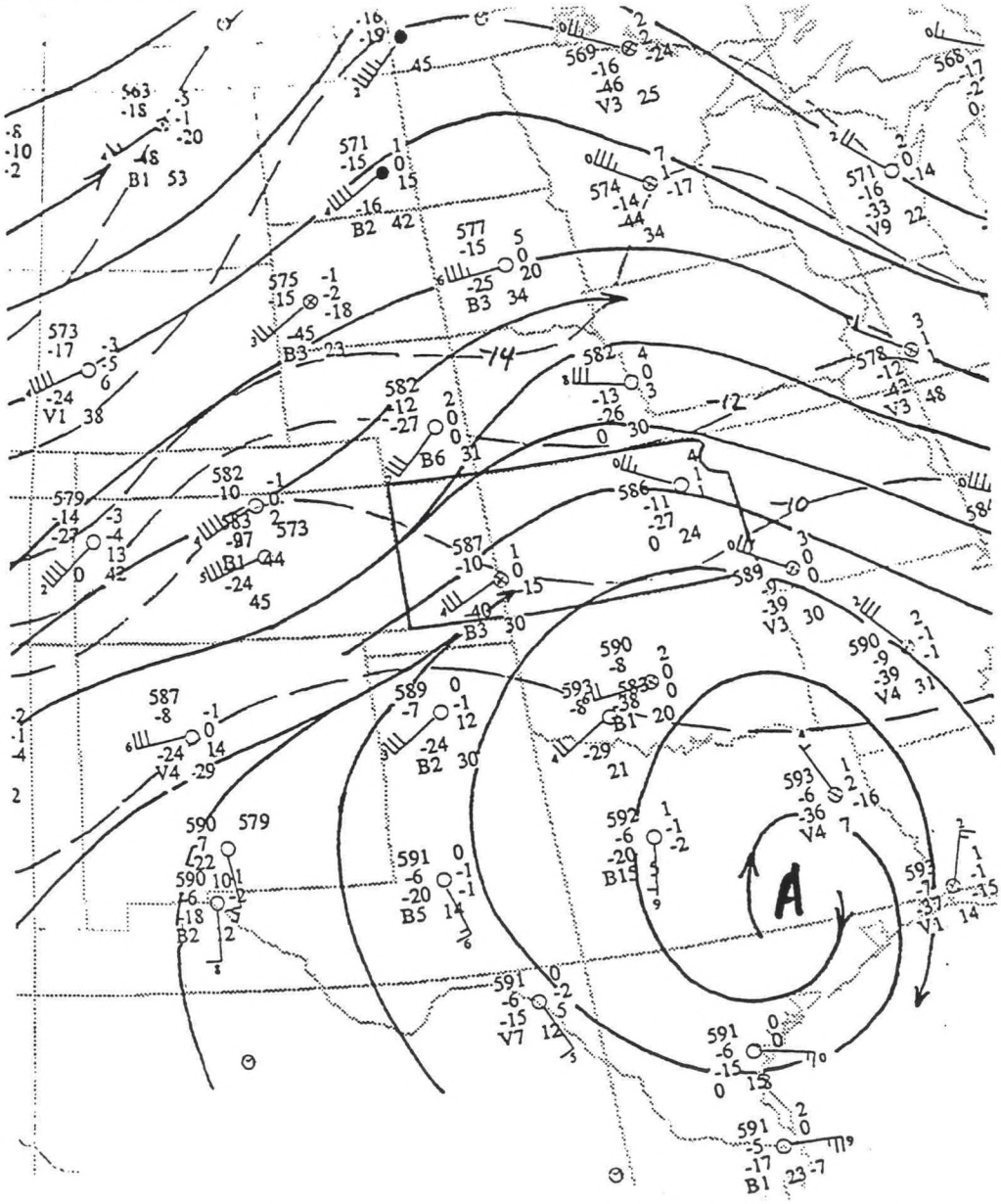

Figure 1. 500-mb streamlines and isotherms (°C), 1200 UTC 21 September 1993.

Further aloft at 250-mb, the axis of the polar jet stream extended from the southern Plateau across northern Kansas into northern Illinois (Figure 2). A wind speed maximum of 90 knots was analyzed across central Utah.

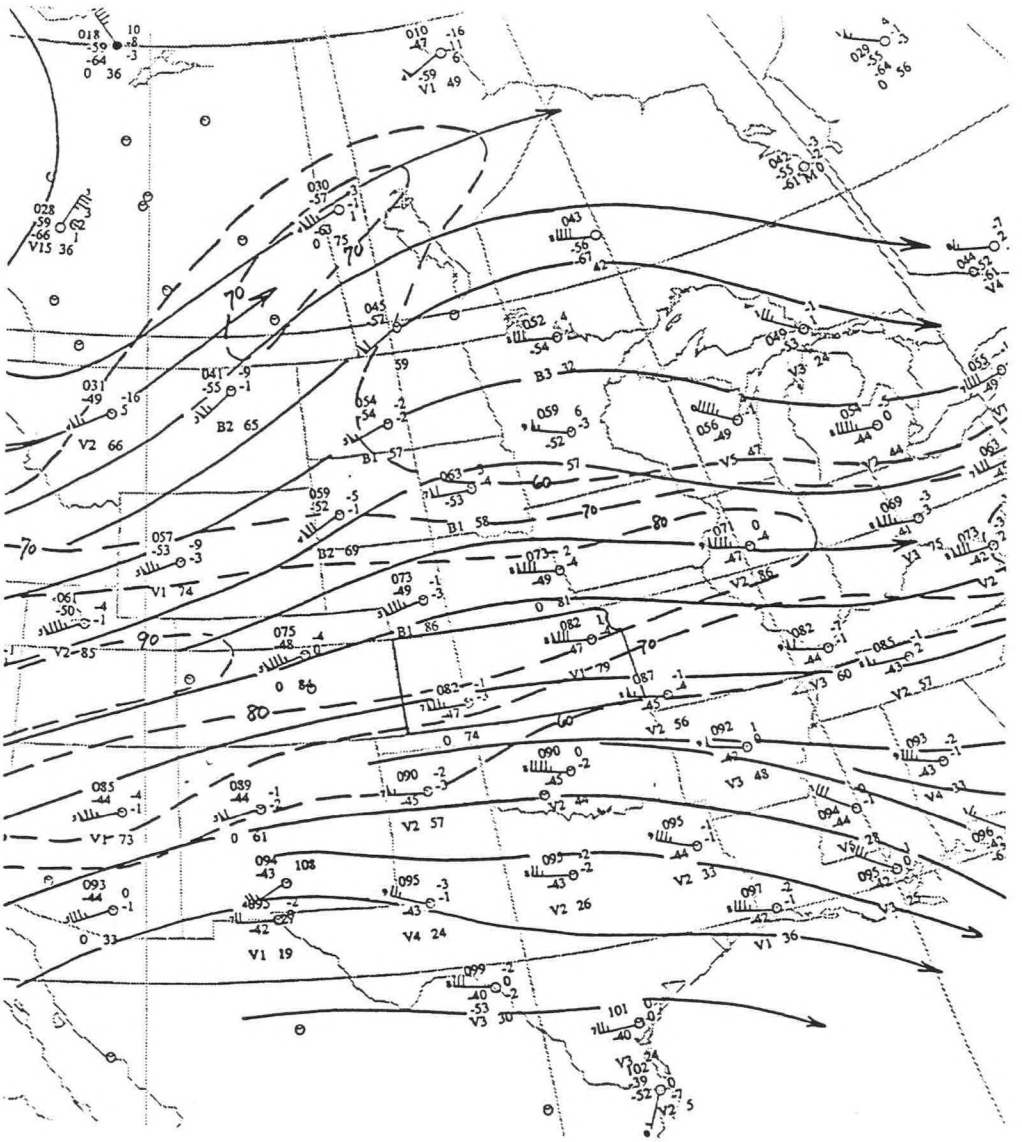

Figure 2. 250-mb streamlines and isotherms (°C), 1200 UTC 21 September 1993.

Several studies (Doswell 1987, and Barnes 1985) have demonstrated the relationship between synoptic-scale forcing and subsequent mesoscale events. Environmental modifications created by factors, such as temperature and moisture advection or dynamic quasi-geostrophic forcing of vertical motion fields, contribute to the support of deep moist convection, which may be initiated by mesoscale events. In this particular case, such dynamic and thermodynamic processes apparently were strong contributing factors toward the modification of the air mass over northeast Kansas.

In response to the backing mid and upper tropospheric winds working into the High Plains, surface pressure gradients were increasing, allowing southerly winds over all of Kansas strengthen. The remains of a weak anticyclone over southern Iowa forced cooler air at low levels into western Missouri. This resulted in a distinct zone of boundary layer frontogenesis, as discussed by Keyser, et al (1987) using the basic concepts of atmospheric frontogenesis as envisioned by Petterssen (1956).

Model gridded data at the sigma(S)-982 level of the NGM at 1200 UTC 21 September (initialized time) was analyzed using PCGRIDDS to illustrate the frontogenic processes present. Reverse arrows in Figure 3b are the dilatation axii of model total wind while dashed lines are isotherms. The parallel nature of the thermal field to the dilatation axii suggest strong frontogenic processes at this level. Solid lines are an analysis of the scalar frontogenesis function. It is clear that the surface boundary across northeast Kansas, Figure 3a, lies within an axis where frontogenic forcing is maximized.

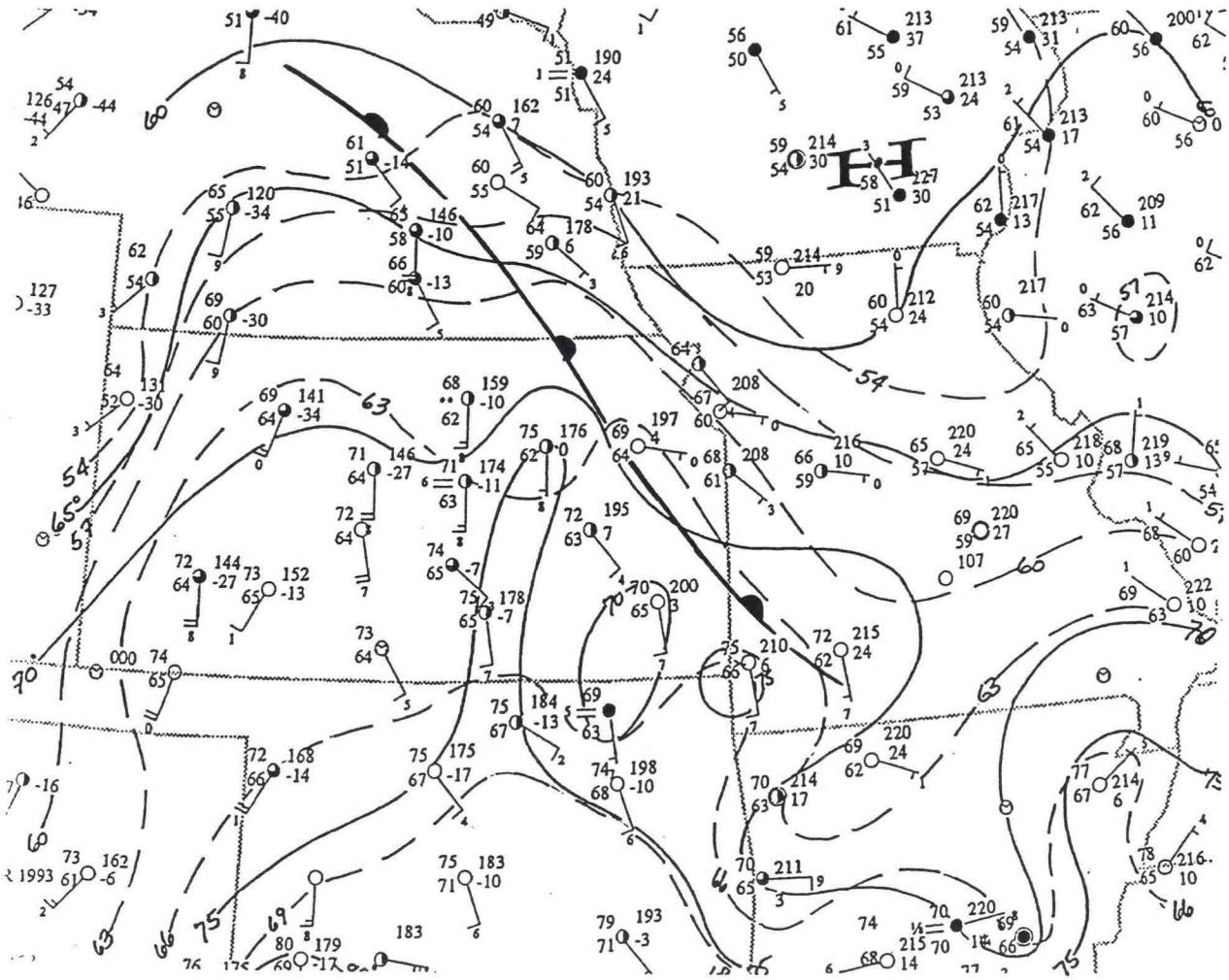

Figure 3a. Surface analysis, 1500 UTC 21 September 1993. Solid lines are isotherms (°F), dashed are isodrosotherms (°F).

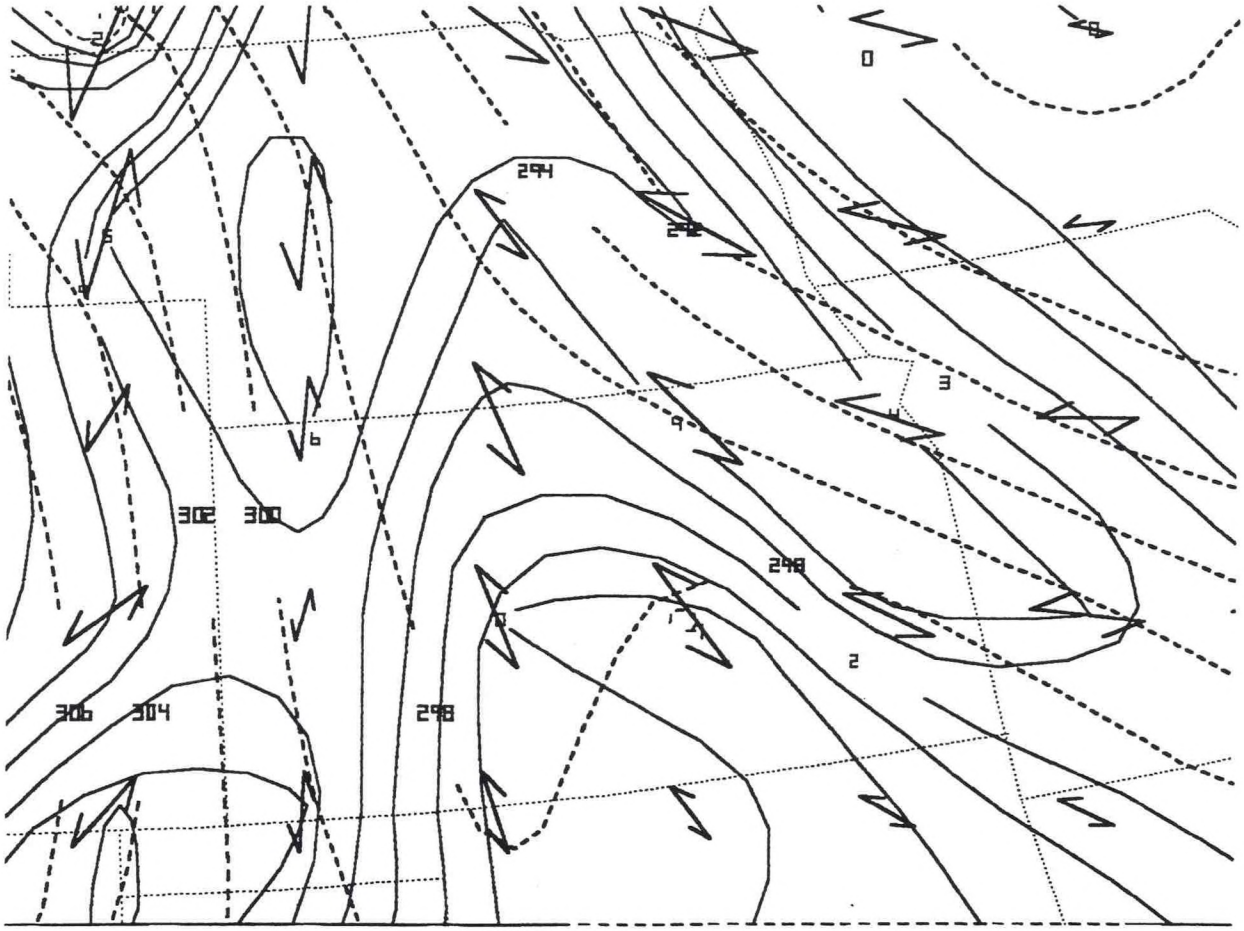

RAFS:LVL=S982:LYR=1000/ 500:FHR= 0 :FHRS= 0/ 12::FILE=se219312.rfs
93/ 9/21/12--CLR3 SSUM SNEG SMLT WSTD

RAFS:LVL=S982:LYR=1000/ 500:FHR= 0 :FHRS= 0/ 12::FILE=se219312.rfs
93/ 9/21/12--CLR3 VNEG LAST&

RAFS:LVL=S982:LYR=1000/ 500:FHR= 0 :FHRS= 0/ 12::FILE=se219312.rfs
93/ 9/21/12--DASH CLR7 THTA CIN2&

RAFS:LVL=S982:LYR=1000/ 500:FHR= 0 :FHRS= 0/ 12::FILE=se219312.rfs
93/ 9/21/12--DNEG SNEG SDVC 2 SMLT MGRD THTA SDIF DVRG WIND&

Figure 3b. Analysis of scalar frontogenesis (solid line) from NGM model gridded data at sigma-layer 982, 1200 UTC 21 September 1995. Potential temperature (dashed) and dilitation axes of total wind (reverse arrows) are overlaid. Units for frontogenesis are 10^{-10}°K/(ms).

While strengthening baroclinicity was evident at the lowest levels, it faded rapidly with height, virtually disappearing in this region at 850-mb. Nonetheless, in the boundary layer where thermal gradients were tightening, moisture gradients were also increasing. The same deformative wind field advecting warmer air into northeast Kansas was also bringing increase moisture. Low level destabilization accelerated during the mid day hours, 1500-1800 UTC, as surface dew points rose 5°-8°F over eastern Kansas to the west of the quasi-stationary frontal zone. Directional confluence also continued near and just west of the frontal zone.

Convection developed at the apex of the thermal axis near CNK before 1500 UTC. It propagated eastward along the crest of the surface thermal ridge, intersecting the increasingly pronounced moisture axis between TOP and CNK.

During the next 6-8 hours, the supercell tracked more and more toward the right, progressing directly along the frontal discontinuity (Figure 3a). As can be seen from examining Figure 4, the front remained essentially stationary through the entire event although the pressure gradient across it continuously strengthened. Surface pressures fell during the day in southeast Kansas while rising east of the boundary in western Missouri. For example, the surface pressure differential between Springfield (SGF), Missouri and Emporia (EMP), Kansas rose from 2.0-mb at 1500 UTC to 5.2-mb at 2100 UTC. This supports a continued intensification of the low level pressure gradient in line with boundary layer frontogenesis diagnosed with this boundary at 1200 UTC.

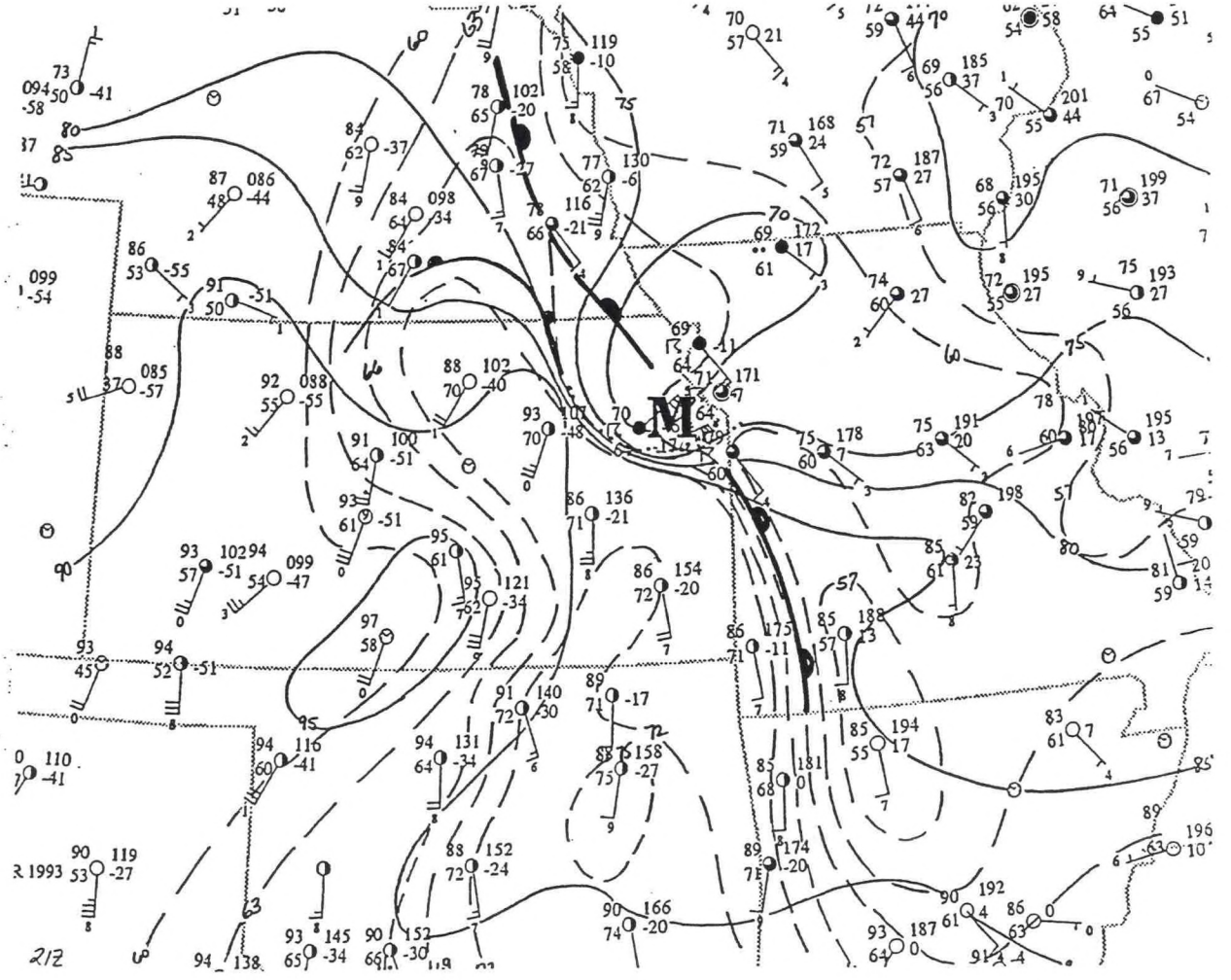

Figure 4. Surface analysis, 2100 UTC 21 September 1993. Solid lines are isotherms (°F), dashed are isodrosotherms (°F).

The track of the supercell is seen in Figure 5. Hail (▲) and tornado (T) reports are noted. Numerous reports of straight line wind damage were also received especially east of Topeka. The southern portion of the mesocyclone circulation passed directly over Topeka. Relationship to the path of the storm to the pre-existing boundary is plainly evident.

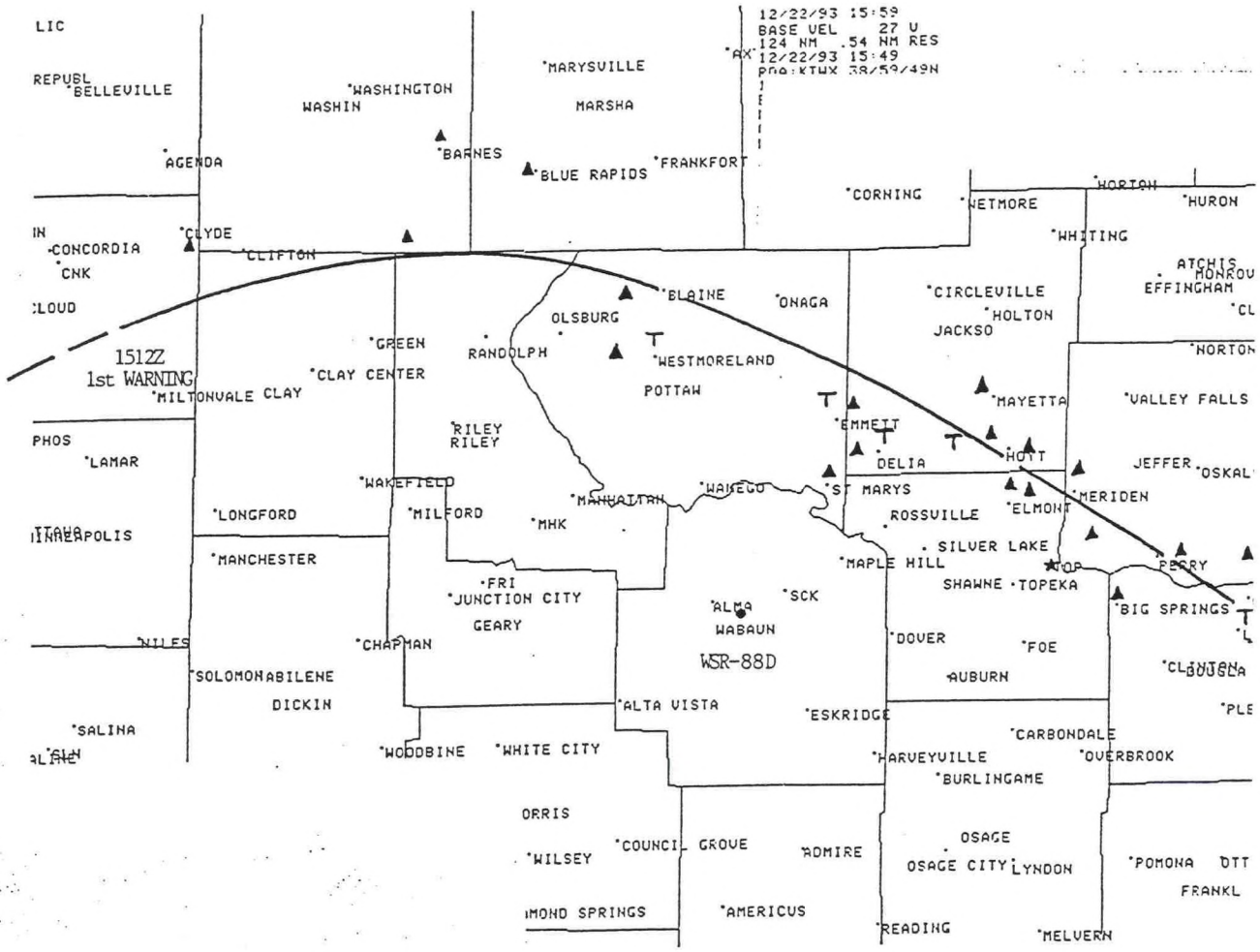

Figure 5. Track of mesocyclone across northeast Kansas, September 21, 1993. Hail reports denoted by ▲, tornado (F0) denoted by T.

A. Environmental Changes

While boundary layer frontogenesis was a contributing factor given the proximity of the surface discontinuity, it appeared that a more important factor was the rapid destabilization from below in the form of boundary layer sensible heat and moisture fluxes near CNK. That was coupled with a weak mid tropospheric short wave trough translating over the area from the west. During the mid morning hours (1500 UTC), strong surface heating through a narrow zone from Wichita (ICT) to Manhatten (MHK), Kansas was augmented by rapidly increasing low level dew points and increasing surface winds.

Upper air and satellite data revealed a weak short wave trough at 1200 UTC moving into northcentral Kansas, along the southern flank of a jet streak. NGM gridded model output was able to resolve this feature using 500-300-mb layer convergence of Q-vectors, Figure 6 (dash denotes convergence). (Q-vector divergence has been directly related to quasi-geostrophic forcing mechanisms through its relation to the ω-equation (Hoskins et al. 1978)). Subsequent studies have linked synoptic-scale ascent as denoted by Q-vectors to air mass modification and support of deep convection. We can surmise, therefore, a zone of rising motion was occurring at mid levels across eastern Kansas during the morning hours resulting in cooling aloft and further destabilization of the column.

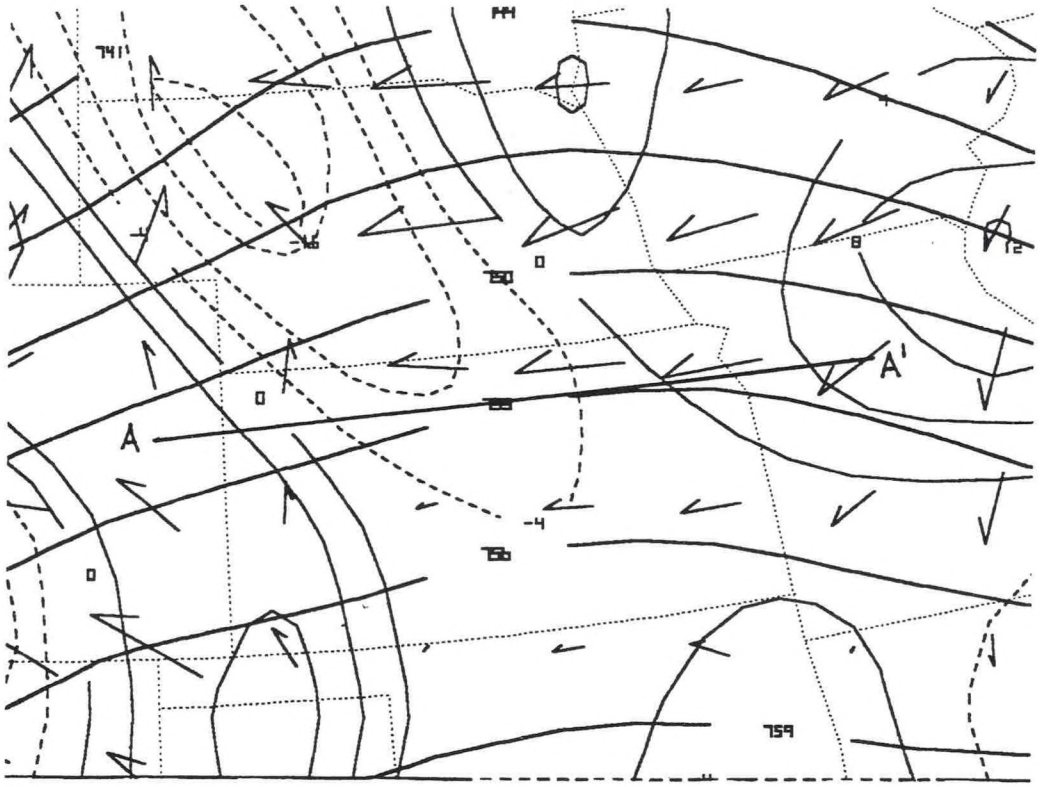

RAFS:LVL= 400:LYR= 500/ 300:FHR= 0 :FHRS= 0/ 24::FILE=se219312.rfs 93/ 9/21/12--CLR6 SNEG

RAFS:LVL= 400:LYR= 500/ 300:FHR= 0 :FHRS= 0/ 24::FILE=se219312.rfs 93/ 9/21/12--DVRG LAST DNEG&

RAFS:LVL= 400:LYR= 500/ 300:FHR= 0 :FHRS= 0/ 24::FILE=se219312.rfs 93/ 9/21/12--HGHT&

Figure 6. Divergence of 500-300-mb layer-Q vectors (units 10^{-16} mb $^{-1}s^{-3}$) from the NGM analysis valid 1200 UTC 21 September 1993. Convergence is dashed.

Confirmation of these processes can be seen in a gridded data cross section taken at 1200 UTC along 39°N through northern Kansas, Figure 7 (Figure 6 shows a cross section line). Solid contours represent temperature advection by the total wind, while dashed are flux divergence of mixing ratio by the wind (negative denotes convergence). The cooling aloft, concentrated at 400-mb and about 250-mb is mirrored below by warming at 700-mb. Through advective processes the column was becoming destabilized just west of CNK, where initial development occurred about 1430 UTC. Perhaps more significant is the strong concentrated convergent flux of moisture in the lowest layers. This injection of moisture would add considerable buoyancy to the boundary layer and provide the fuel for subsequent convective activity.

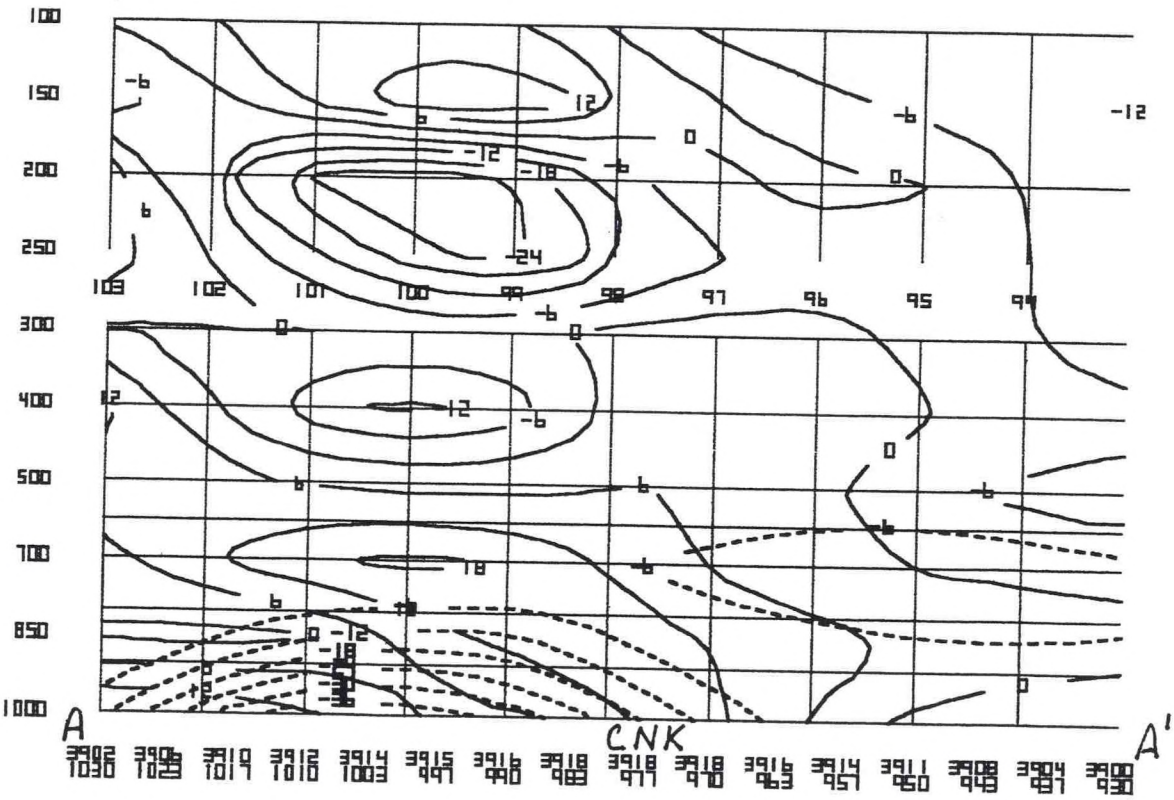


```
 RAFS:Lon/Lat103/39-> 93/39:FHR=  0 :FHRS=  0/ 24::FILE=se219312.rfs
93/ 9/21/12--ADVT TEMP WIND&

 RAFS:Lon/Lat103/39-> 93/39:FHR=  0 :FHRS=  0/ 24::FILE=se219312.rfs
93/ 9/21/12--SDVR MIXR WIND DNEG LT00&
```

Figure 7: Cross section along line A-A' of Figure 6. Solid lines are advection of temperature by the total wind (units 10^{-4} °C/s). Dashed represent flux convergence of mixing ratio by the total wind (units 10^{-4} $gkg^{-1}s^{-1}$).

GOES-7 water vapor satellite imagery at 1200 UTC revealed a short wave trough moving through northwest Kansas, embedded along the axis of the 250-mb jet. The 400-mb data (not shown) shows the feature best and is supported by a shallow thermal trough. By 1500 UTC (Figure 8) imagery depicted the leading edge of this feature, as defined by a dark zone extending from north-central Kansas northward into Nebraska, just west of CNK. The coincident nature of strong low level forcing via sensible heat and moisture flux plus movement of a definable upper tropospheric short wave trough into the same location supports a coupled destabilization within the column.

The TOP sounding at 1200 UTC was characterized by a non-threatening list of traditional severe weather parameters. These included CAPE = 34 J/Kg, Lifted Index = 0, 0-3 km storm-relative helicity = 93 and EHI = .02. These values likely reflected, to a great extent, air mass characteristics of the cooler air over northwest Missouri.

Mixing and advective processes during the subsequent six hours significantly modified this environment. Using observed temperature/dew point values in the inflow region of the storm (prior to its passage at Topeka), a modified "proximity" sounding can be constructed. Figure 9 illustrates the change. Now the CAPE = 2930 J/Kg, Lifted Index = -9, and EHI = 5.40!

Equally significant were changes of the hodograph parameters. Using low-level wind data from the WSR-88D at about 1630 UTC (when the RDA site was in the mesocyclone inflow zone) and adjusting for a right deviant motion of 295°/14 kt (obtained from observed storm motion), the 0-3 km storm-relative helicity jumps from 93 (1200 UTC TOP RAOB) to 366. The hodograph, Figure 10, resembles those associated with long lived supercell storms as described by Leftwich (1990). The low level inflow of about 30 kt from 150° agrees well with observed surface wind at TOP prior to passage of the mesocyclone at the station.

Profiler data (not shown) from the proximity sites of Hillsboro (HBR), Kansas and Lathrop (LTH), Missouri revealed 500-mb winds consistently at 20-25 m/s suggesting a 0-5 km speed shear of about 20m/s within the ambient environment.

A contributing, and not insignificant, element in the events to unfold was the existence of the stationary frontal boundary across northeast Kansas (Figure 3). While apparently shallow in depth, frontogenic forcing along its axis acted as a focus zone for tightening moisture and temperature gradients through the day. Results of the modifications are evident in the thermodynamic and hodograph changes described above.

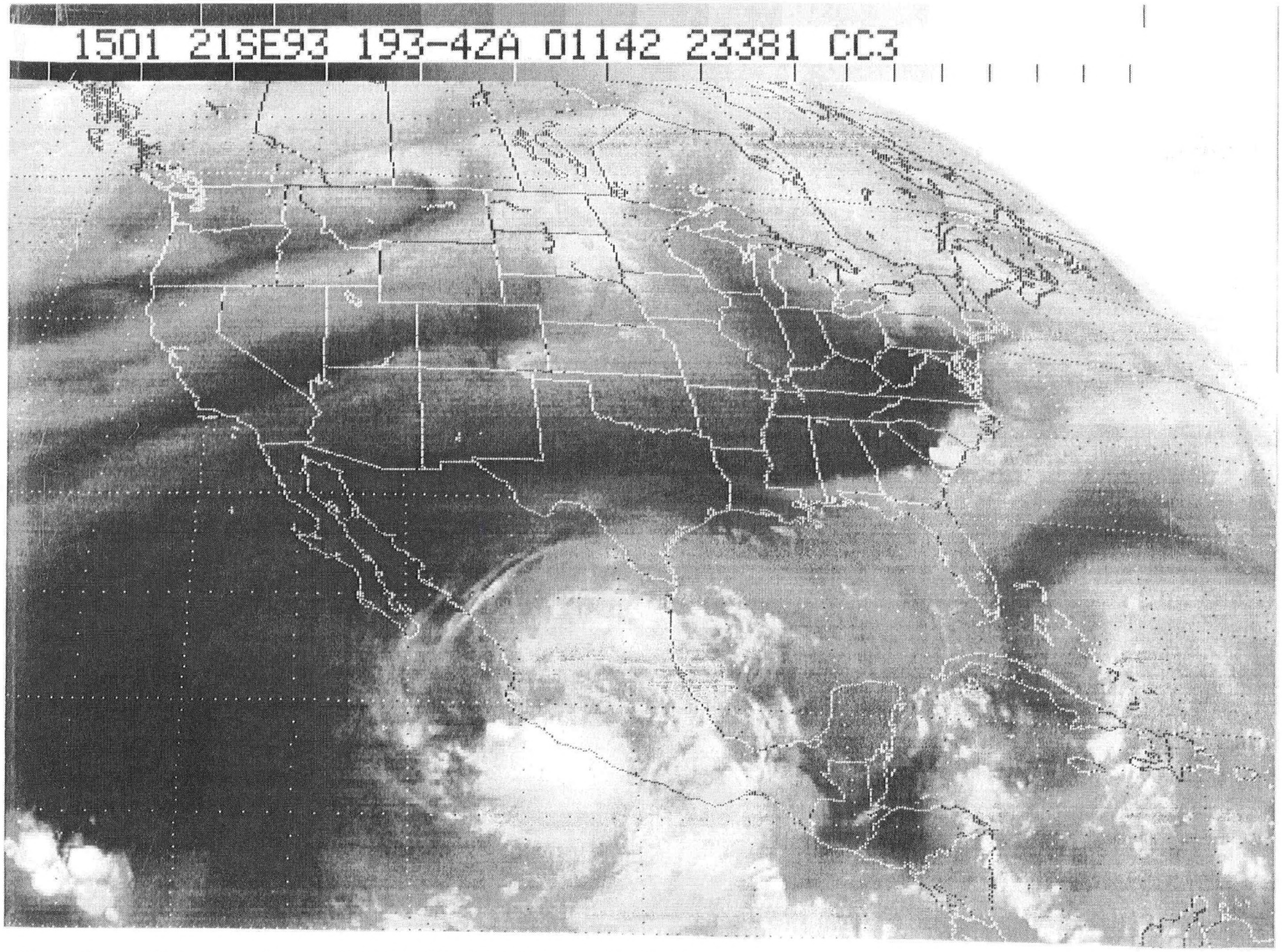

Figure 8. Water vapor image, GOES 7, 1501 UTC 21 September 1993.

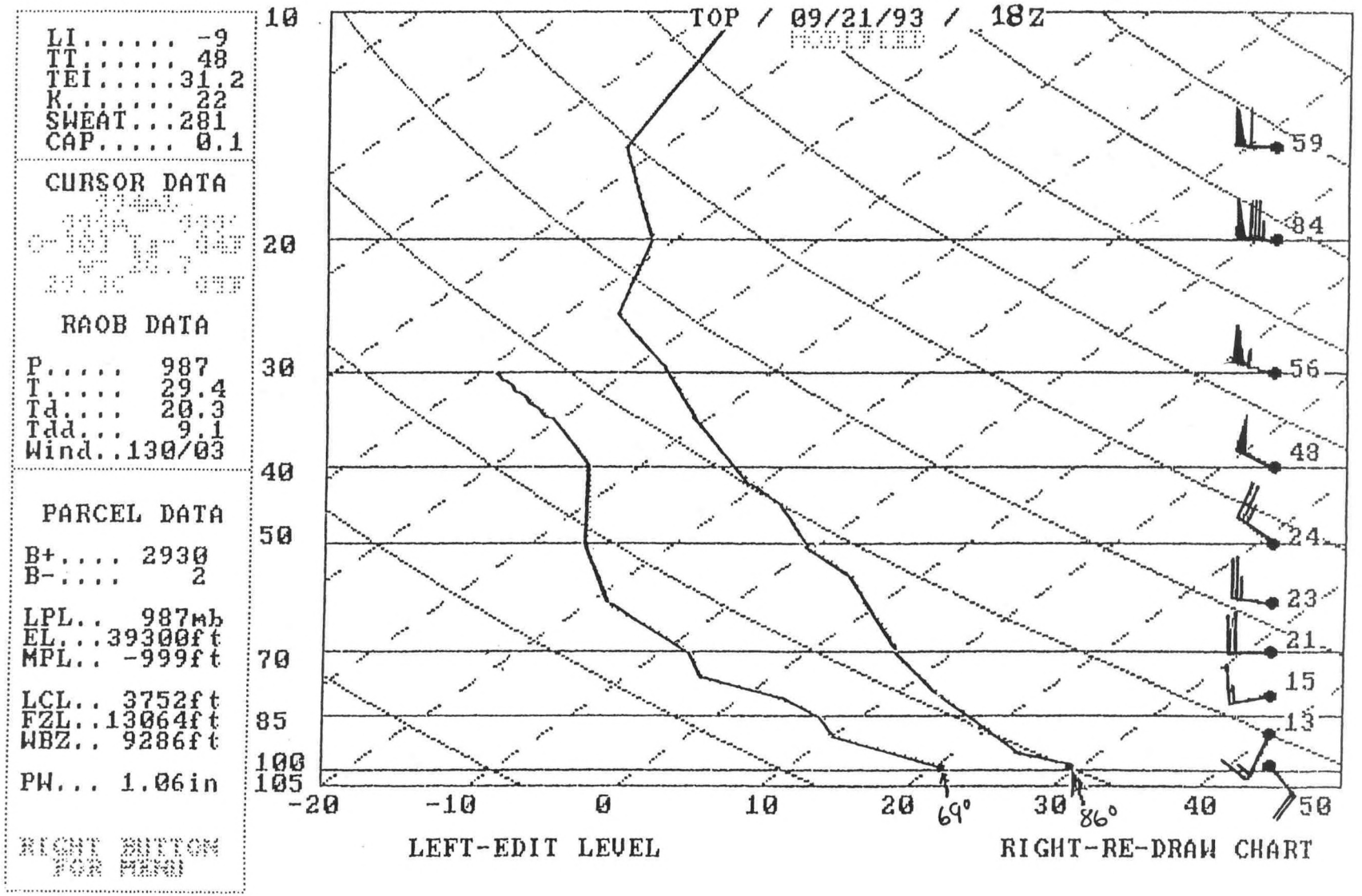

Figure 9. Modified Topeka sounding at 1800 UTC 21 Septmber 1993. Observed surface temperature (°F) and dew point (°F) are noted at 1000-mb. Other parameters are conventional MKS units, as given by the SHARP program (Hart and Korotky 1991).

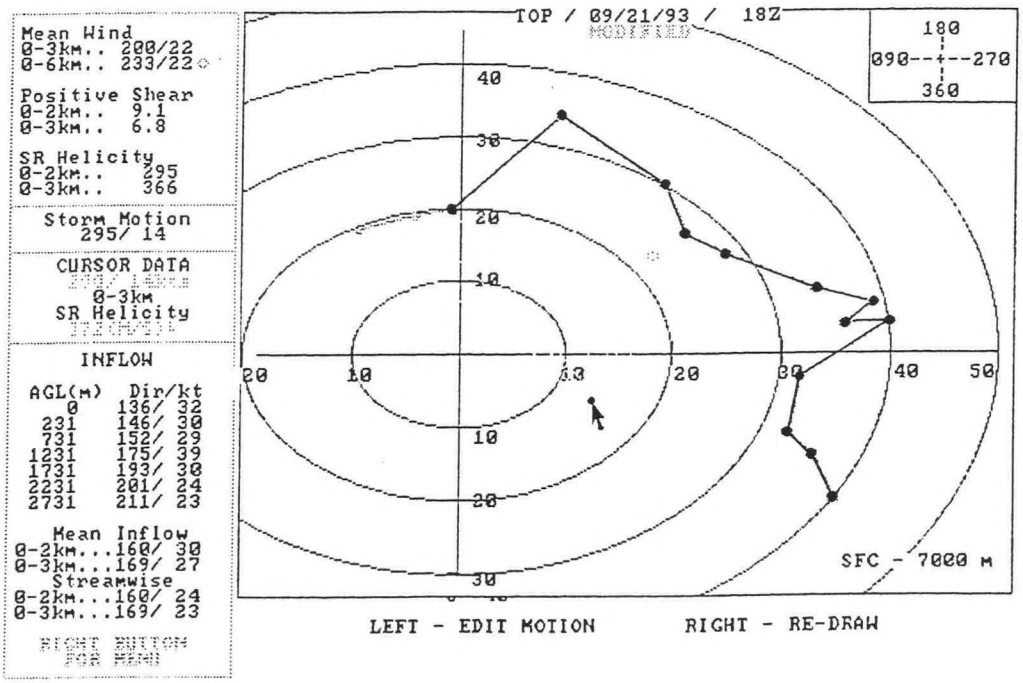

Figure 10. Modified Topeka hodograph at 1800 UTC 21 September 1993. Actual storm motion noted by ⁻. Helicity units are m^2s^{-2} and shear is represented by $10^{-3}s^{-1}$.

GOES water vapor images also showed a persistent "C"-shaped dark band along the upwind edge of the cirrus anvil. It is identical to the phenomena described by Ellrod (1990). The features appeared early in the development, about 1600 UTC, which closely corresponded to the initial warning issued by WSO CNK at 1512 UTC and persisted until 2300 UTC after which rapid weakening (on radar) occurred. The persistence of this dark zone feature during the entire time of severe weather occurrence is testimony to the prolonged strength and severity of this storm.

B. Model Gridded Data Insights

The manipulation of model gridded data via PCGRIDDS allows detailed investigation of meteorological processes unavailable until recently. Given that it is model output and not the real atmosphere, investigation of this data using the NGM data set from both 21/0000 UTC and 21/1200 UTC revealed some intriguing insights (some of which have been discussed above). The NGM was used because sigma levels are available in lower elevations and 21/0000 UTC output was investigated to determine prognostic value beginning at 12 hours.

While a much larger area in the central Plains was outlooked for severe storms after 21/1200 UTC, attention was focused in northcentral Kansas at 1200 UTC. We wanted to see, in hindsight, whether initial and forecast model

gridded data could have been used to isolate this area as a potential for severe convection. Given the premise that contributing factors, at least initially, were destabilization of the column through sensible heat (temperature) and moisture flux below and cooling aloft, various parameters were examined. One concern was the shallow nature of the heat/moist layer with respect to model resolution.

Some of these results, from 21/1200 UTC initial NGM model data are detailed above. In Figure 11, the 12 hour NGM forecast valid 21/1200 UTC of the Laplacian of low level thermal advection overlaid with Laplacian of 400-mb thermal advection is shown. For the lowest level the 1000-850-mb thickness was used for the computation of lower tropospheric temperature advection, to give a broader representation of conditions. A maxima of positive rate of temperature change (Laplacian is a second order differential denoting the spatial **rate** of change of a scalar, in this case temperature) in the low levels, solid line, is overlaid by a minima (dashed) over northeast Kansas. This is the exact area where severe convection was initiated about 21/1430 UTC. As a check, the 500-300-mb thickness was substituted for 400-mb layer and results were very close.

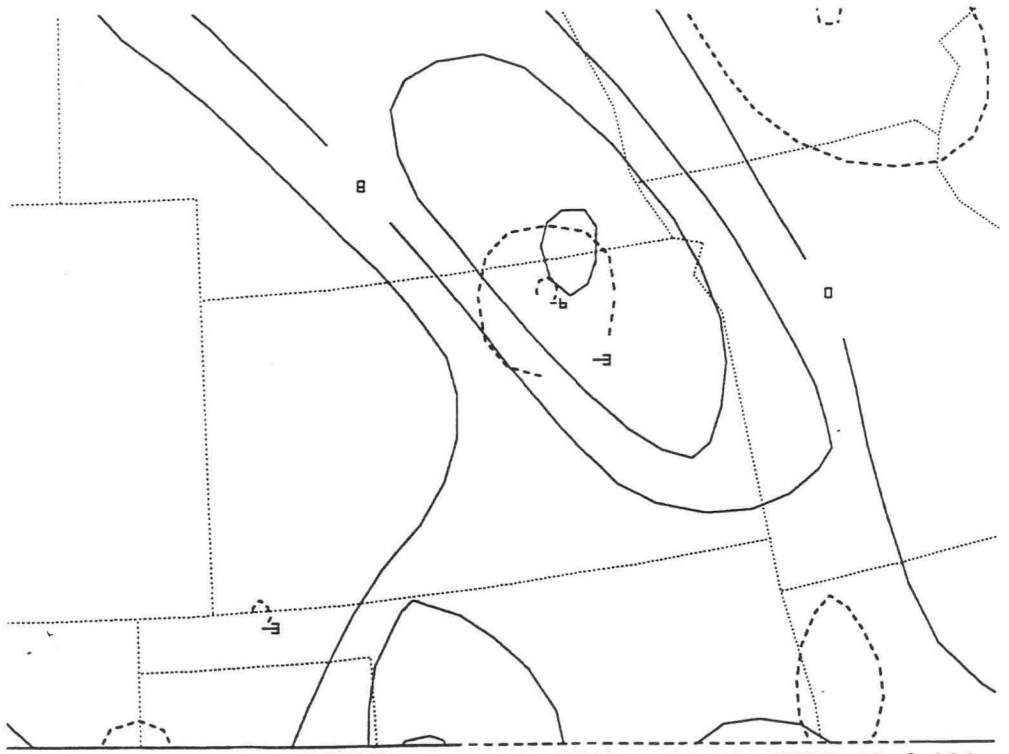

RAFS:LVL= 400:LYR=1000/ 850:FHR= 12 :FHRS= 0/ 24::FILE=00rfs921
93/ 9/21/ 0--SNEG DVRG GRAD ADVT HGHT LDIF WKNT LAVE DNEG GT00

RAFS:LVL= 400:LYR=1000/ 850:FHR= 12 :FHRS= 0/ 24::FILE=00rfs921
93/ 9/21/ 0--SNEG DVRG GRAD ADVT TEMP WKNT DNEG LT00&

Figure 11. Laplacian (greatest rate of change) of temperature advection at 400-mb (dash = cooling) (units are 10^{-14} °C $m^{-2}s^{-1}$) and Laplacian of 1000-850-mb thickness change (units are $10^{-14}m^{-1}s^{-1}$) (solid = warming or increasing thickness). Twelve hour forecast of gridded model data, valid 1200 UTC 21 September 1993 from initial NGM valid 0000 UTC 21 Sept. 1993.

The initial data at 21/1200 UTC, (Figure 6) had the greatest lift and implied cooling aloft west of the first development, but it was poised to advect into northcentral Kansas very soon. In either case (from initial or 12 hour prog), gridded model data was able to isolate this small area prone to thermal destabilization.

Isentropic analysis has gained increased usage. Could this view of the atmosphere give a similar result? In Figure 12, the 300°K surface is depicted through the 880-960-mb pressure levels. The maximum lift (dry adiabatic ascent along the isentropic surface, dashed) is seen along the thermal axis (pressure ridge) at the eastern edge of the increased southerly gradient. The zone is virtually identical to the location where thermal destabilization is occurring through the deeper column.

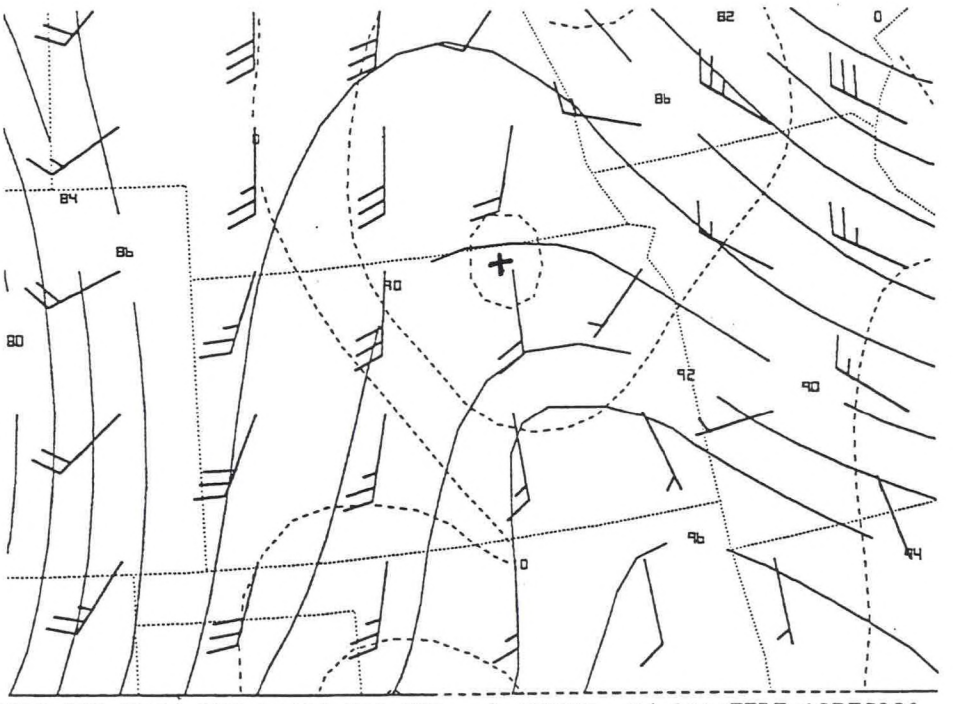

Figure 12. Winds and pressure surfaces along the 300K isentropic surface at 1200 UTC 21 September 1993, from NGM model gridded data. Dashed analysis denotes rising motion (pressure advection) along same surface (maxima = +). Units of pressure are in mb (solid), wind speed is in knots (1 full barb = 10 kt, half barb = 5 kts) and adiabatic omega is 10^{-4}mbs^{-1} (dashed lines).

3. RADAR AND STORM EVOLUTION

A. Pre-Supercell Stage

The first development along the warm front was associated with altocumulus castellanus (ACCAS) observed over northcentral Kansas shortly after 1300 UTC. The ACCAS developed into high based thunderstorms west of Concordia around 1400 UTC, as detected by the TOP WSR-88D (KTWX) operating in "clear air mode", VCP 32. By 1500 UTC, the storm was becoming rapidly organized as it moved into an increasingly moist low level environment. It quickly became severe with the first warning issued at 1512 UTC by CNK. Most severe reports during this early stage were of three-quarter to one inch hail.

B. Supercell Stage

The storm first began displaying supercell characteristics, including a weak echo region (WER), and a persistent rotating updraft (mesocyclone), around 1720 UTC, shortly after Figure 13. Base reflectivity data revealed a pendant on the southwest quadrant of the storm. Storm-Relative velocity Map (SRM) data showed an intensifying cyclonic convergent rotation in the mid levels of the storm (17,000 to 27,000 ft). All height references are AGL. The mesocyclone had rotational velocities (V_r) of 30 kts in the mid-levels with weak cyclonic rotation noted at 0.5° (4000 ft).

The outflow boundary, which had been responsible for initiating new convection along the southwest quadrant, began to wrap into the storm circulation by 1743 UTC. The wrap up of this low-level boundary into the storm's updraft region appeared to be associated with the intensification of the mesocyclone. This feature acted as a source of baroclinically generated horizontal vorticity similar to numerical simulations shown by Klemp (1987). Observations recorded by Maddox et al (1980) suggested the warm front across northeast Kansas could also have provided a source of baroclinically generated horizontal vorticity. By 1743 UTC, V_r increased to 40 to 45 kts (at 15,000 ft) with the diameter of the mesocyclone core decreasing to 2 nm. A brief F0 tornado was reported north of Westmoreland at 1750 UTC.

Between 1743 and 1830 UTC the supercell appeared to remain quasi-steady state. Four panel reflectivity displays showed the presence of a BWER in the mid-levels of the storm (20,000 to 30,000 ft). A reflectivity pendant at the 0.5° elevation slice continued to extend to the southwest. SRM data[1] continued to show a mesocyclone with V_r of 20 to 30 kts at 0.5° (approximately 3000 ft) with 30 to 40 kt V_r in the mid-levels (15,000 to 25,000 ft).

---

[1]SRM data as computed by the WSR-88D algorithm was misleading during much of event due to an unrepresentative storm motion used in SRM calculation. This made velocity interpretation difficult during the event.

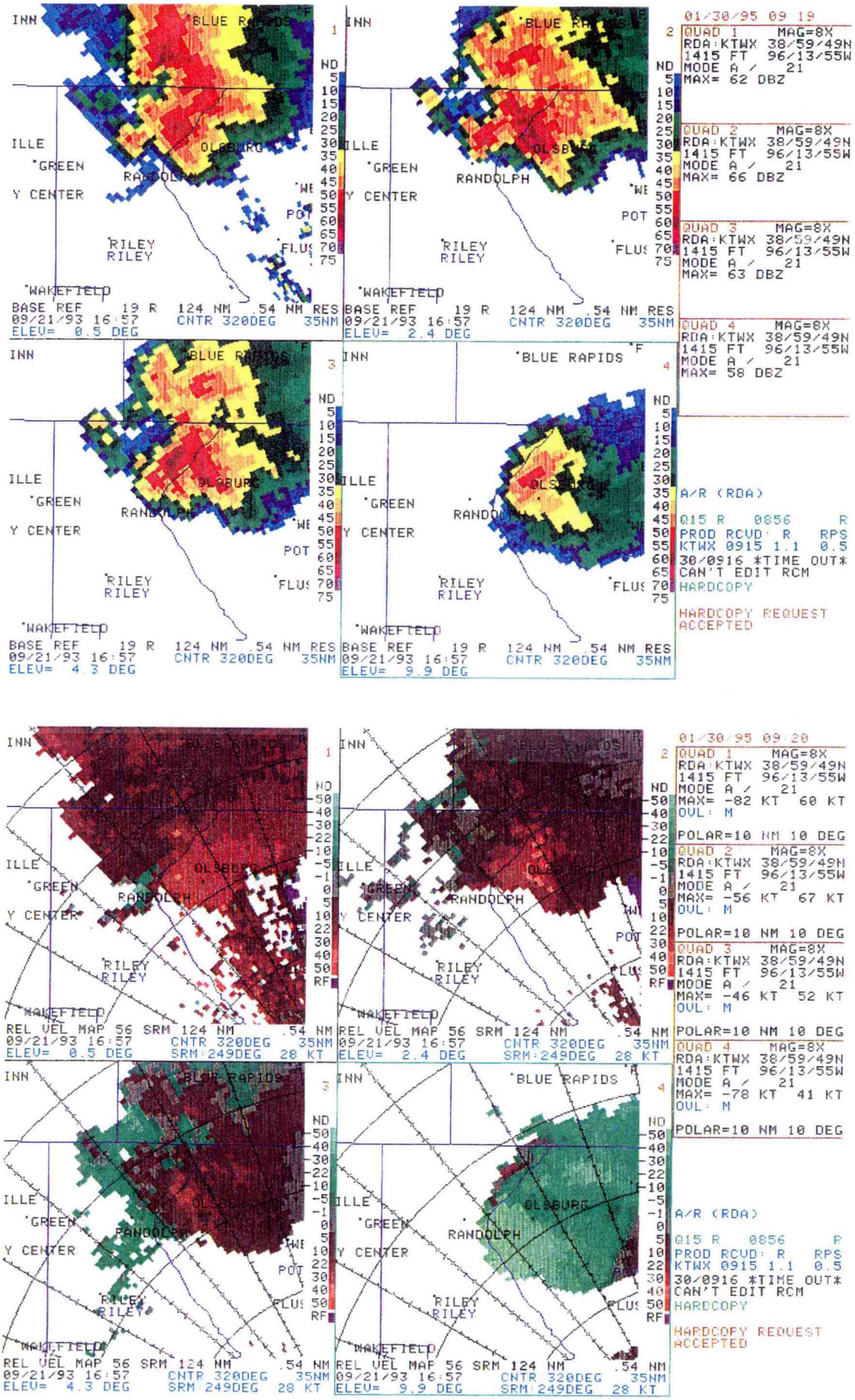

Figure 13. Base reflectivity (top 4-panel) and storm relative velocity map (lower 4-panel) at 1657 UTC 21 September 1993 from Topeka WSR-88D, KTWX.

A second low-level spin-up apparently occurred between 1830 and 1900 UTC[2] as the BWER collapsed. Base reflectivity data from 0.5° at 1909 UTC (Figure 14) showed the "hook" had wrapped into the storm. SRM data indicated a corresponding increase in low-level V_r. The 3 nm diameter mesocyclone core had V_r of 55 kts at 0.5°. Between 1840 and 1935 UTC, the storm produced three F0 tornadoes.

Through 2000 UTC, the storm continued to display classic supercell characteristics such as a sharp inflow reflectivity notch and overhang along the southern flank, BWER, and coherent (in time and space) rotational signature as it moved southeast along the well established nearly stationary front.

C. Transition Stage

Between 2000 and 2030 UTC, the storm appeared to gradually evolve into a hybrid supercell with multicellular characteristics. Forward speed slowed to less than 10 kts. The 0.5° reflectivity hook disappeared and the mid-level overhang became less pronounced. The 0.5° echo took on an oblong shape with upper elevation slices showing several separate high reflectivity cores and rotational centers suggesting multiple updrafts were present in the storm (Figure 15). A pronounced outflow boundary formed on the storm's southern flank and began to accelerate away from the storm. SRM data showed strong obstacle flow in the mid levels of the storm (20,000 ft). The low-level circulation weakened with V_r dropping to 25 to 30 kts. However, the mid-level (13000 to 20000 ft) mesocyclone remained strong with V_r averaging around 40 kts. During this time period, numerous reports of wall clouds and funnels were received, but no tornadoes were sighted. Rainfall rates increased rapidly from 1.9 inches per hour at 1800 UTC to 3.1 inches per hour at 2000 UTC.

D. High-Precipitation Supercell Stage

HP supercell characteristics began to become evident as the storm approached Lawrence around 2100 UTC. Between 2110 and 2122 UTC (Figure 16) the gust front to the south (seen in the 0.5° reflectivity slice) retreated toward the storm as it began to acquire a kidney bean shape. The inflow region was surrounded by strong reflectivity gradients at 0.5° and capped by 50+ dBZ echo at 25000 ft. These reflectivity features suggested that the BWER had reformed[3].

Between 2100 and 2115 UTC, the mesocyclone shifted from the southwest quadrant of the storm (classic) to the front flank (HP). Reposition of the mesocyclone and primary inflow region toward the forward quadrant of a

---

[2]Reflectivity and velocity data were not available for the 1830 to 1900 GMT time period due to a failure at the RDA.

[3]Due to limitations caused by the RPS list being used, the BWER was not always evident in four panel reflectivity data.

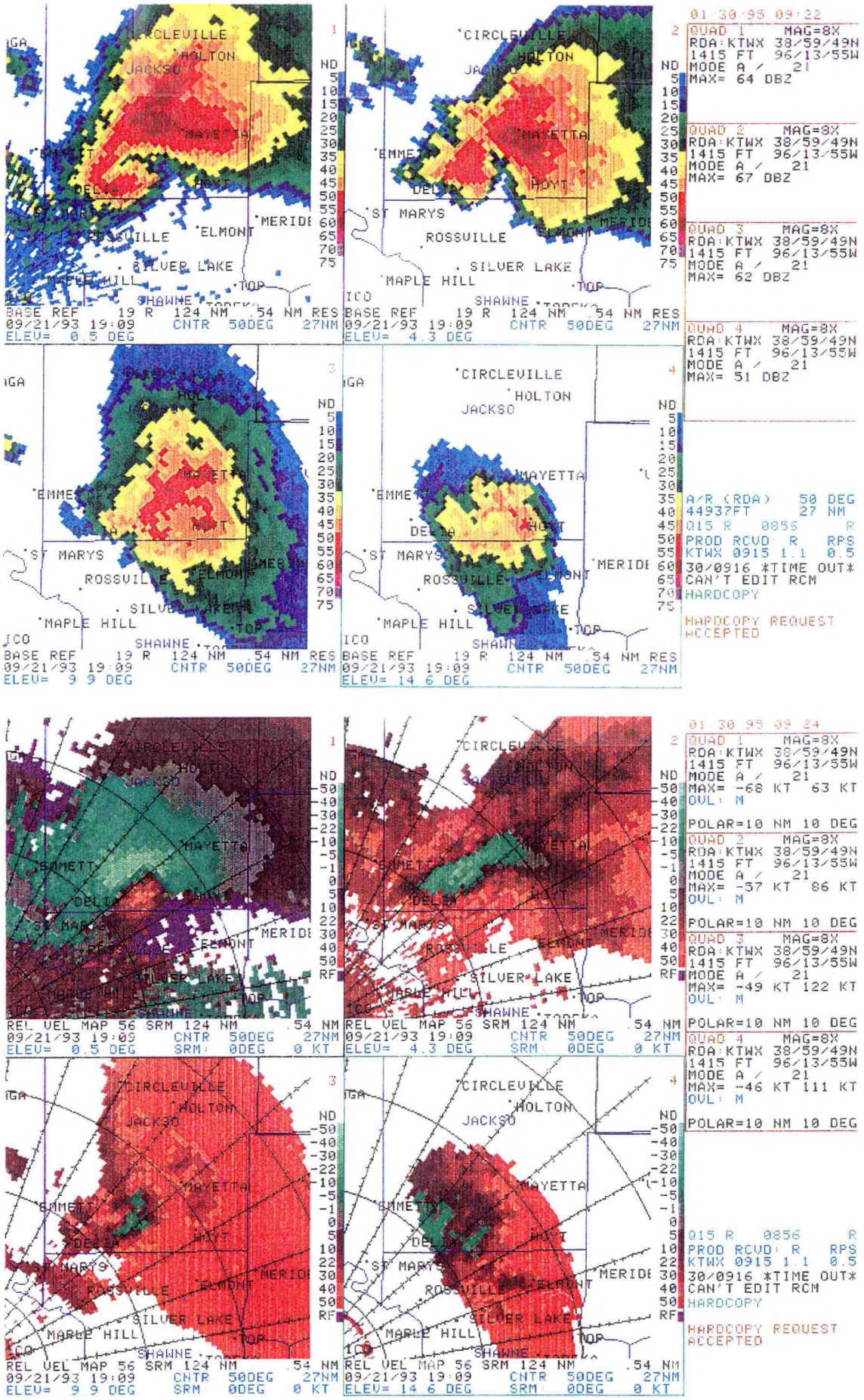

Figure 14. Base reflectivity (top 4-panel) and storm relative velocity map (lower 4-panel) at 1909 UTC 21 September 1993 from Topeka WSR-88D.

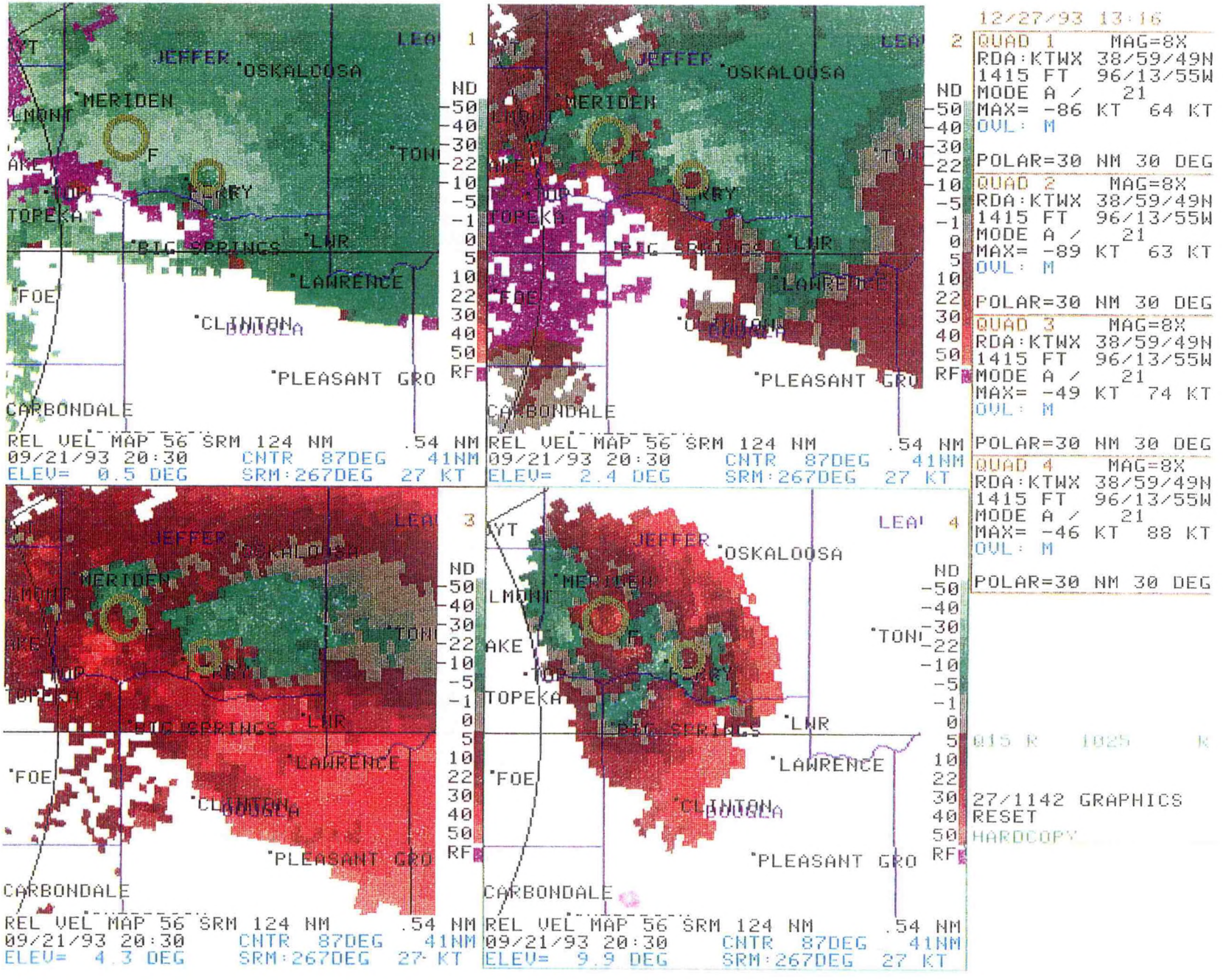

Figure 15. Storm relative velocity map 2030 UTC 21 September 1993 from Topeka WSR-88D. Circles on image are detected mesocyclones (by 88D algorithm).

supercell is consistent with characteristics shown to be associated with HP supercells (Przybylinski et al. 1993). In addition, the mid level reflectivity pattern assumed a "S" shape through the mid levels (Figure 16, slice 4.3°) as precipitation was being redistributed by the mesocyclone circulation.

Between 2110 and 2122 UTC, a rapid intensification of the mesocyclone occurred, possibly in response to the baroclinically generated horizontal vorticity, supplied as the storm overtook the outflow boundary, was tilted into the vertical by the updraft. During this period, V_r at 0.5° increased from 35 kts to 45 kts while V_r at 15,000 ft increased from 30 to 50 kts. The diameter of the mesocyclone core also contracted from 5 to 3 nm during this interval.

A brief F0 tornado along with wind gusts to 76 mph occurred at the Lawrence airport at 2120 UTC (about the time of Figure 16). Significant wind damage was reported in the city of Lawrence between 2120 and 2135 UTC, as the fat hook reflectivity pattern moved over the city. Careful examination of Figure 16 shows an erosion of the rear reflectivity at 0.5° which becomes a distinct concave signature at 2.4° and 4.3° elevation slices. These are consistent with development of a Rear Inflow Notch (RIN) associated with the Rear Flank Downdraft (RFD) and supports the potential for the damaging surface winds which occurred. Additionally, SRM data from 0.5° showed a divergent signature just south of Lawrence, a further indication of damaging surface winds.

E. Bow Echo Stage

Around 2145 UTC, the storm began its final transformation. The RIN noted well aloft a short time earlier over Lawrence began descending. Around 2200 UTC, a bowing of the 0.5° echo was noted. SRM data from this time showed a well developed Rear Inflow Jet descending from the upper levels (rear flank) to the lower levels (front flank) of the storm. At 0.5°, the SRM data indicated a well developed divergent signature at the leading edge of the storm with a rotating comma head on its northern end of the echo. By 2218 UTC, Figure 17, a series of well defined Rear Inflow Notches (weak echo channels) could be seen on the rear flank of the 0.5° echo. Base velocity images showed 36 to 50 kt outflow occurring ahead of these notches. Numerous occurrences of hail and damaging winds associated with this bow echo were reported in the southwestern suburbs of Kansas City.

F. Radar Summary

During the time period from 1500 UTC 21 September to 0000 UTC 22 September, Doppler data revealed a progression of evolutionary changes in a long-lived supercell which moved across northeast Kansas. The early stages were marked by strong low-level reflectivity gradients surrounding the storm's inflow region and a large (5-7 nm) mid-level reflectivity overhang along the

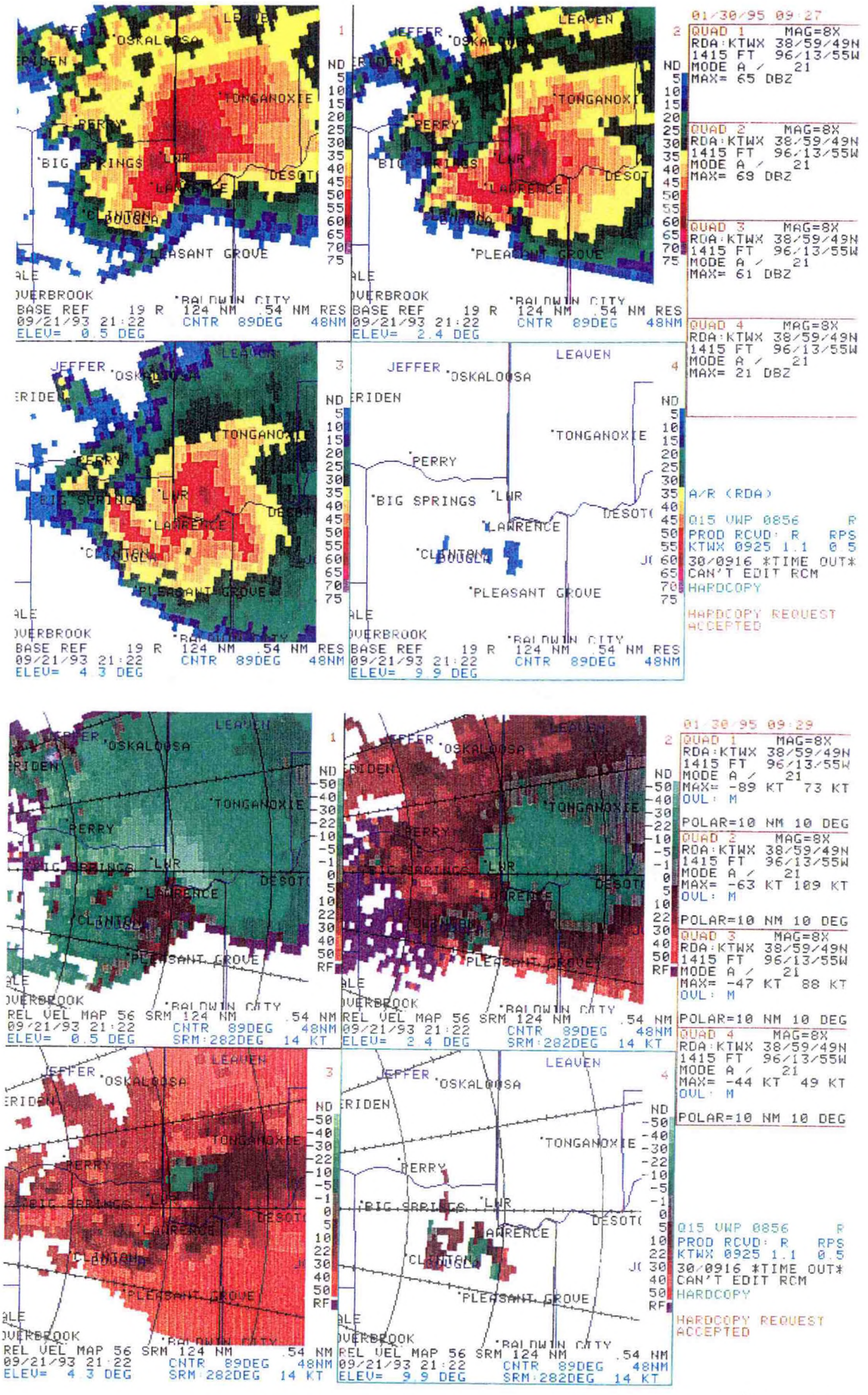

Figure 16. Base reflectivity (top 4-panel) and storm relative velocity map (lower 4-panel) at 2122 UTC 21 September 1993 from Topeka WSR-88D.

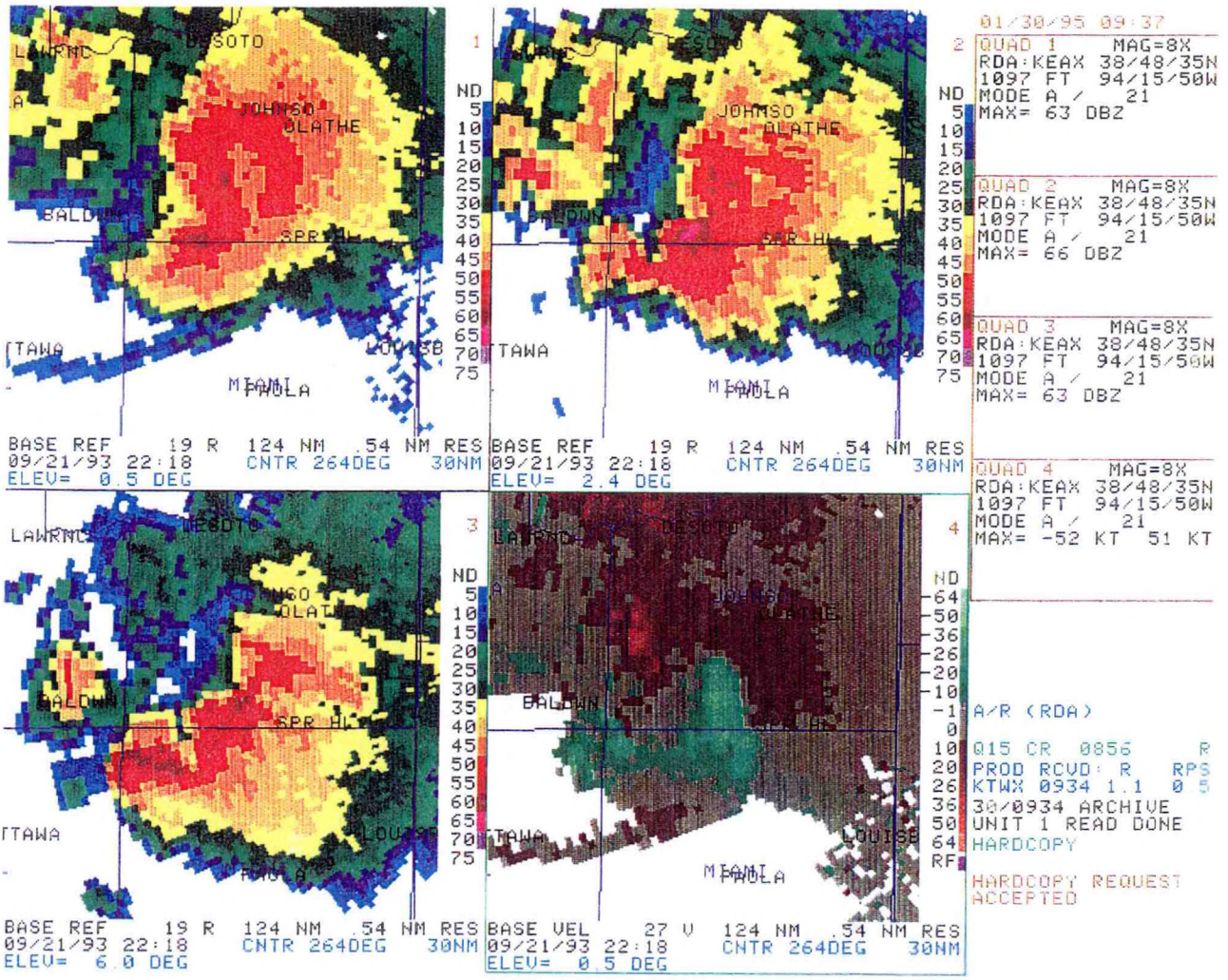

Figure 17. Base reflectivity and base velocity at 2218 UTC 21 September 1993 from Topeka WSR-88D.

storm's southern flank. In classic supercell fashion, the majority of large hail reports occurred along the southern edge of the 0.5° echo in the updraft region and beneath the attendant mid level overhang.

Even though the supercell exhibited most reflectivity characteristics associated with tornadic mesocyclone thunderstorms, only four brief F0 tornadoes were reported. SRM data showed a persistent well developed mid-level mesocyclone with V_r averaging 40 kts during this period of the storm's life.

During the evolution from a classic to a HP supercell, the reflectivity vault and overhang disappeared only to reform once the HP configuration was obtained. Based on conceptual models of HP storms (Przybylinski et al. 1993) an "S" shaped reflectivity structure present during the HP phase suggested the presence of a deep, organized mesocyclone which redistributed the precipitation fields within the storm.

The BWER noted on the storm's inflow flank was a reflection of the storm's strong, rotating updraft while the RIN observed along the trailing flank was a reflection of the RFD and accelerated rain cooled air. This RIN, associated with the Rear Inflow Jet, descended toward the front flank of the storm causing the low-level echo to acquire a bow shape during its final stages.

4. SUMMARY AND DISCUSSION

The supercell which developed over northcentral Kansas during the morning of September 21, 1993, formed in a sheared environment destabilized by strong low-level warm air and moisture advection, as well as cooling aloft associated with a migratory short wave trough. Low-level convergence along a well developed quasi-stationary frontogenic surface boundary provided the mesoscale focus to initiate thunderstorm development.

The resulting convection coalesced into a single supercell which existed for nearly nine hours. It evolved through a full spectrum structural changes, initially possessing a classic supercell identity, then a HP look before "winding down" as a bow echo. During its life span, a variety of severe weather occurred but no long track tornadoes formed. Lightning was observed originating from the anvil northeast of Kansas City during the late afternoon.

A possible explanation for the lack of long track tornadoes might be found in examining the 3 to 7 km wind shear. Brooks et al. (1993) suggests that with low shear conditions (0.005 s^{-1}) in the mid levels (3-7 km) the formation of the low-level meso-cyclone should be rapid but short lived. Under moderate shear conditions (0.010 s^{-1}) the formation of the low-level mesocyclone should be slower, but its should also be more persistent. In this case the 3-7 km shear values ranged from 0.004 s^{-1} at 1700 UTC to 0.006 s^{-1} at 2000 UTC, based on profiler data. This suggests that the low-level mesocyclone circulations which formed should have been transitory in nature.

While the supercell as a reflectivity entity remained well defined during an extended period, progressing through the phases described above, detectable mesocyclonic circulations periodically "spun up" and decayed. Given the marginal shear environment, as defined by Brooks, one can visualize a series of mesocyclone swirls being generated by the persistent updraft in an ambience of rich vorticity periodically being doused by descending precipitation and cold air. This may have contributed to the production of numerous F0 tornadoes but none of the "long track" variety.

In addition, a portion of the recurrent intensification of the supercell complex can probably be attributed to interactions along the frontogenic synoptic frontal zone, as well as varying degrees of horizontal vorticity created low level baroclinicity generated from the advancing rain shield.

Observationally this type of metamorphasis from classic or HP supercell to eventual bow echo or straight line wind event is apparently not uncommon in eastern Kansas. The massive amount of water entrained into these systems and associated evaporative cooling seems to become the eventual controlling process, providing a large pool of cold air which becomes manifest in the formation of bow echoes or straight line winds.

5. ACKNOWLEDGEMENTS

We would like to thank Ron Przybylinski (SOO), WSFO St. Louis, and Ed Berry, CRH SSD, for their extensive help in the review and preparation of this manuscript.

6. REFERENCES

Barnes, S.L., 1985: Omega Diagnostics as a Supplement to LFM/MOS Guidance in Weakly Forced Convective Situations. *Mon. Wea. Rev.*, **113**, 2122-2141.

Brooks, H.E., C.A. Doswell III, and R.B. Wilhelmson, 1993: The Role of the Mid-Level Winds in the Evolution and Maintenance of Low-level Mesocyclones. *Mon. Wea. Rev.*, **122**, 126-136.

Doswell, C.A. III., 1987: The Distinction between Large-Scale and Mesoscale Contribution to Severe Convection: A Case Study Example. *Wea. and Forecasting*, **2**, 3-16.

_____, A.R. Moller, and R.W. Przybylinski, 1990: A unified set of conceptual models for variations on the supercell theme. *Preprints, 16th Conference Severe Local Storms*, Kananaskis Park, Canada, AMS (Boston), 40-45.

Ellrod, G.P., 1990: A Water Vapor Image Feature Related to Severe Thunderstorms. *Nat. Wea. Digest*, **15**, 21-29.

Hart, J.A., and W.D. Korotky, 1991: The SHARP Workstation v1.50. A Skew T/hodograph analysis and research program for IBM and compatible PC. Users Manual. DOC/NOAA/NWS Forecast Office, Charleston, WV, 62pp.

Hoskins, B.J., I. Draghici, and H.C. Davies, 1978: A new look at the ω-equation. *Quart. J. Roy. Meteor. Soc.*, **104**, 31-38.

Johns, R.H., J.M. Davies, and P.W. Leftwich, 1990: An Examination of the Relationship of 0-2 km AGL "Positive" Wind Shear to Potential Buoyant Energy in Strong and Violent Tornado Situations. *Preprints, 16th Conf. Severe Local Storms*, Kananaskis Park, Canada, AMS (Boston) 593-598.

_____, C.A. Doswell III, 1992: Severe Local Storms Forecasting. *Wea. and Forecasting*, **4**, 588-612.

Keyser, D., M.J. Reeder, R.J. Reed, 1987: A Generalization of Petterssen's Frontogenesis Function and Its Relation to the Forcing of Vertical Motion. *Mo. Wea. Rev.*, **116**, 762-780.

Klemp, J.B., 1987: Dynamics of Tornadic Thunderstorms. *Ann. Rev. Fluid Mech.*, **19**, 369-402.

Leftwich, P.W. Jr., 1990: On the Use of Helicity in Operational Assessment of Severe Local Storm Potential. *Preprints, 16th Conf. Severe Local Storms*, Kananaskis Park, Canada, AMS (Boston), 306-310.

Maddox, R.A., L.R. Hoxit, and C.F. Chappell, 1980: A Study of Tornadic Thunderstorm Interactions with Thermal Boundaries. *Mon. Wea. Rev.*, **108**, 322-336.

Petterssen, S., 1956: *Weather Analysis and Forecasting*, Vol. 1, Motion and Motion Systems. 2nd ed. McGraw-Hill, 428 pp.

Przbylinski, R.W., T.J. Shea, D.L. Ferry, E.H. Goetsch, R. Czys, and N.E. Wescott, 1993: Doppler radar observations of high precipitation supercells over the mid-Mississippi valley region. *Preprints, 17th Conf. Severe Local Storms*, St. Louis, MO, AMS (Boston), 158-163.

NWS CR 47 Practical Application of a Graphical Method of Geostrophic Wind Determination. C.B. Johnson, November 1971 (COM 71-01084).

NWS CR 48 Manual of Great Lakes Ice Forecasting. C. Robert Snider, December 1971 (COM 72-10143).

NWS CR 49 A Preliminary Transport Wind and Mixing Height Climatology, St. Louis, Missouri. Donald E. Wuerch, Albert J. Courtois, Carl Ewald, Gary Ernst, June 1972 (COM 72-10859).

NWS CR 50 An Objective Forecast Technique for Colorado Downslope Winds. Wayne E. Sangster, December 1972 (COM 73-10280).

NWS CR 51 Effect on Temperature and Precipitation of Observation Site Change at Columbia, Missouri. Warren M. Wisner, March 1973 (COM 73-10734).

NWS CR 52 Cold Air Funnel Clouds. Jack R. Cooley and Marshall E. Soderberg, September 1973, (COM 73-11753/AS).

NWS CR 53 The Frequency of Potentially Unfavorable Temperature Conditions in St. Louis, Missouri. Warren M. Wisner,October 1973.

NWS CR 54 Objective Probabilities of Severe Thunderstorms Using Predictors from FOUS and Observed Surface Data. Clarence A. David, May 1974 (COM 74-11258/AS).

NWS CR 55 Detecting and Predicting Severe Thunderstorms Using Radar and Sferics. John V. Graff and Duane C. O'MalleyJune 1974 (COM 74-11335/AS).

NWS CR 56 The Prediction of Daily Drying Rates. Jerry D. Hill, November 1974 (COM 74-11806/AS).

NWS CR 57 Summer Radar Echo Distribution Around Limon, Colorado. Thomas D. Karr and Ronald L. Wooten, November 1974 (COM 75-10076/AS).

NWS CR 58 Guidelines for Flash Flood and Small Tributary Flood Prediction. Lawrence A. Hughes and Lawrence L. Longsdorf, October 1975 (PB247569/AS)

NWS CR 58 (Revised) March 1978 (PB281461/AS)

NWS CR 59 Hourly Cumulative Totals of Rainfall - Black Hills Flash Flood June 9-10, 1972. Don K. Halligan and Lawrence L. Longsdorf, April 1976 (PB256087).

NWS CR 60 Meteorological Effects on the Drift of Chemical Sprays. Jerry D. Hill, July 1976 (PB259593).

NWS CR 61 An Updated Objective Forecast Technique for Colorado Downslope Winds. Wayne E. Sangster, March 1977 (PB266966/AS).

NWS CR 62 Design Weather Conditions for Prescribed Burning. Ronald E. Haug, April 1977 (PB268034).

NWS CR 63 A Program of Chart Analysis (With Some Diagnostic and Forecast Implications). Lawrence A. Hughes, December 1977 (PB279866/AS).

NWS CR 64 Warm Season Nocturnal Quantitative Precipitation Forecasting for Eastern Kansas Using the Surface Geostrophic Wind Chart. Wayne E. Sangster, April 1979 (PB295982/AS).

NWS CR 65 The Utilization of Long Term Temperature Data in the Description of Forecast Temperatures. Arno Perlow,November 1981 (PB82 163064).

NWS CR 66 The Effect of Diurnal Heating on the Movement of Cold Fronts Through Eastern Colorado. James L. Wiesmueller, August 1982 (PB83 118463).

NWS CR 67 An Explanation of the Standard Hydrologic Exchange Format (SHEF) and Its Implementation in the Central Region. Geoffrey M. Bonnin and Robert S. Cox, April 1983 (PB83 193623).

NWS CR 68 The Posting of SHEF Data to the RFC Gateway Database. Geoffrey M. Bonnin, April 1983 (PB83 222554).

NWS CR 69 Some Basic Elements of Thunderstorm Forecasting. Richard P. McNulty, May 1983 (PB83 222604).

NWS CR 70 Automatic Distribution of AFOS Products Created at the NOAA Central Computer Facility via Hamlet (RJE) PunchStream. Billy G. Olsen and Dale G. Lillie, November 1983 (PB84 122605).

NWS CR 71 An Investigation of Summertime Convection Over the Upper Current River Valley of Southeast Missouri. Bartlett C. Hagemeyer, July 1984 (PB84 222389).

NWS CR 72 The Standard SHEF Decoder Version 1.1. Geoffrey M. Bonnin, August 1984 (PB85 106508).

NWS CR 73 The Blizzard of February 4-5, 1984 Over the Eastern Dakotas and Western Minnesota. Michael Weiland, October 1984 (PB85 120087).

NWS CR 74 On the Observation and Modeling of the Slope Winds of the Upper Current River Valley of Southeast Missouri and Their Relationship to Air-Mass Thunderstorm Formation. Bartlett C. Hagemeyer, June 1985 (PB85 226926/AS).

NWS CR 75 Complete Guide to Canadian Products in AFOS. Craig Sanders, July 1985 (PB85 228153/AS).

NWS CR 76 The Reliability of the Bow Echo as an Important Severe Weather Signature. Ron W. Przybylinski and William J. Gery, September 1985 (PB86 102340).

NWS CR 77 Observation of Bow Echoes with the Marseilles Radar System. John E. Wright, Jr., September 1985 (PB86 102340).

NWS CR 78 Statistical Analysis of SHEF Coding Errors. Robert S. Cox, Jr., January 1986 (PB86 145141).

NWS CR 79 On the Midwestern Diurnal Convergence Zone on the West Side of the Warm Season Bermuda High. Bartlett C. Hagemeyer, March 1986 (PB86 171378).

NWS CR 80 Some Characteristics of Northeast Kansas Severe Weather 1963-1984. Larry W. Schultz, March 1986 (PB86 173952/AS).

NWS CR 81 The Severe Thunderstorm Outbreak of July 6, 1983 in Southeast Idaho, Western Wyoming and Southwest Montana. Gary L. Cox, April 1986 (PB86 184322/AS).

NWS CR 82 Some Proposals for Modifying the Probability of Precipitation Program of the National Weather Service. Wayne E. Sangster and Michael D. Manker, July 1986 (PB86 226636/AS).

NWS CR 83 Deformation Zones and Heavy Precipitation. Henry Steigerwaldt, August 1986 (PB86 229085/AS).

NWS CR 84 An Overview of the June 7, 1984 Iowa Tornado Outbreak. Charles H. Myers, August 1987.

NWS CR 85 Operational Detection of Hail by Radar Using Heights of VIP-5 Reflectivity Echoes. Richard B. Wagenmaker, September 1987.

NWS CR 86 Fire Weather Verification: The Forecaster Does Make a Difference. Therese Z. Pierce and Scott A. Mentzer, December 1987 (PB88 140744).

NWS CR 87 Operational Use of Water Vapor Imagery. Samuel K. Beckman, December 1987 (PB88 140751).

NWS CR 88 Central Region Applied Research Papers 88-1 Through 88-7. NWS Central Region, Scientific Services Division, May 1988 (PB88-210836).

NWS CR 89 Compendiums of Information for the Missouri Basin River Forecast Center and the North Central River ForecastCenter. NWS Central Region, Scientific Services Division, June 1988 (PB88-226204).

NWS CR 90 Synoptic-Scale Regimes Most Conducive to Tornadoes in Eastern Wyoming -A Link Between the Northern Hemispheric Scale Circulation and Convective-Scale Dynamics. William T. Parker and Edward K. Berry, July 1988 (PB88-231337).

Continued on Back Cover.

NWS CR 91 Heavy Snowfall in Northwest Wyoming. Michael S. Weiland, September 1988 (PB89 109524).

NWS CR 92 On the Utility of a Geographic Information System in Modelling Climatic Suitability. Bartlett C. Hagemeyer, September 1988 (PB89 109516).

NWS CR 93 The Synoptic and Meso-Alpha Scale Meteorology of Wyoming Flash Floods. Joseph A. Rogash, October 1988 (PB89 117709)

NWS CR 94 The Removal of Stagnant Winter Air Masses From Wyomings Wind River Basin. Gary L. Cox and Jeffrey M. Graham, November 1988 (PB89 128664).

NWS CR 95 Floods Along Des Plaines and Fox Rivers: September-October 1986. Thomas L. Dietrich, February 1989 (PB89 152797/AS)

NWS CR 96 A Case Study Evaluation of Satellite-Derived Rainfall Estimates and Their Application to Numerical Model Precipitatio Forecast Verification. Glenn A. Field, May 1989 (PB89 194591).

NWS CR 97 Central Region Applied Research Papers 97-1 through 97-6. NWS Central Region, Scientific Services Division, July 198 (PB89 213375/AS).

NWS CR 98 The Record Rainfall of August 13-14, 1987 at Chicago, Illinois. Paul Merzlock, November 1989.

NWS CR 99 Central Region Applied Research Papers 99-1 through 99-7. NWS Central Region, Scientific Services Division, November 1989 (PB90 151325).

NWS CR 100 A Guide to Forecasters in Judging Weather Impact on Growth Environments and Farm Operations in the Midwest. John W. Kottke, December 1989 (PB90 141011).

NWS CR 101 Numerical Solutions to the Shallow Water Equations as Applied to a Local Meteorological Forecast Problem. Eric R. Thaler, March 1990 (PB90 191230).

NWS CR 102 Postprint Volume National Weather Service Aviation Workshop Kansas City, Missouri, December 10-13, 1991. NWS Central Region, Scientific Services Division, March 1992 (PB92-176148).

NWS CR 103 An Investigation of Two Microburst Producing Storms Using A Microburst Recognition Algorithm. David Eversole, January 1994 (PB94-156577).

NWS CR 104 Lincoln ASOS Temperature Test January 13-15, 1993, Gregory Grosshans and Phil Clark, March 1994 (PB94-159993).

NWS CR 105 Forecasting Snowfall Using Mixing Ratios on an Isentropic Surface "An Empirical Study", Crispin Garcia, Jr, May 1994 (PB94-188760).

NWS CR 106 The Use of Profiler Data for Analysis and Nowcasting of a Winter Season Extratropical Cyclone, Bradley S. Small, June 1994 (PB94-187804).

NWS CR 107 Flood Forecasting for the Lower Missouri River Basin: June - September, 1993, John F. Pescatore, September 1994 (PB95-123568).

NWS CR 108 Heterogeneous Nucleation and its Relationship to Precipitation Type, Gregory Smith, April 1995 (PB95-217170).

NOAA SCIENTIFIC AND TECHNICAL PUBLICATIONS

The National Oceanic and Atmospheric Administration was established as part of the Department of Commerce on October 3, 1970. The mission responsibilities of NOAA are to assess the socioeconomic impact of natural and technological changes in the environment and to monitor and predict the state of tha solid Earth, the oceans and their living resources, the atmosphere, and the space environment of the Earth.

The major components of NOAA regularly produce various types of scientific and technical information in the following kinds of publications.:

PROFESSIONAL PAPERS--Important definitive research results, major techniques, and special investigations.

CONTRACT AND GRANT REPORTS--Reports prepared by contractors or grantees under NOAA sponsorship.

ATLAS--Presentation of analyzed data generally in the form of maps showing distribution of rainfall, chemical and physical conditions of oceans and atmosphere, distribution of fishes and marine mammals, ionospheric conditions,etc.

TECHNICAL SERVICE PUBLICATION--Reports containing data, observations, instructions, etc. A partial listing includes data serials; prediction and outlook periodicals; technical manuals, training papers, planning reports, and information serials; and miscellaneous technical publications.

TECHINCAL REPORTS--Journal quality with extensive details, mathematical developments, or data listings.

TECHNICAL MEMORANDUMS--Reports of preliminary, partial, or negative research or technology results, interim instructions, and the like.

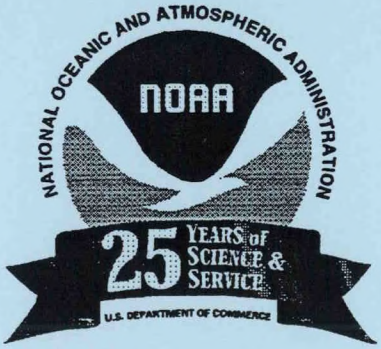

Information on availability of NOAA publication can be obtained from:

NATIONAL TECHNICAL INFORMATIN SERVICE
U.S. DEPARTMENT OF COMMERCE
5285 PORT ROYAL ROAD
SPRINGFIELD, VA 22161